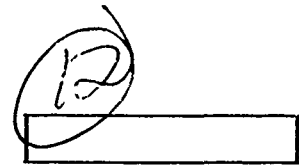


AD A 1 3 0 7 4 3



# **RESEARCH ON FIRE-RESISTANT DIESEL FUEL FLAMMABILITY MITIGATION MECHANISMS**

**INTERIM REPORT  
AFLRL No. 165**

By

**W. D. Weatherford, Jr.**

**D. W. Naegeli**

**U.S. Army Fuels and Lubricants Research Laboratory  
Southwest Research Institute  
San Antonio, Texas**

Under Contract to

**U.S. Army Mobility Equipment Research  
and Development Command  
Materials, Fuels, and Lubricants Laboratory  
Fort Belvoir, Virginia**

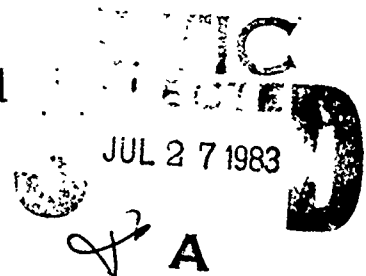
**Contract No. DAAK70-82-C-0001**

Approved for public release; distribution unlimited

December 1982

83 07 26 008

DTIC FILE COPY



### **Disclaimers**

The findings in this report are not to be construed as an official Department of the Army position unless so designated by other authorized documents.

Trade names cited in this report do not constitute an official endorsement or approval of the use of such commercial hardware or software.

### **DTIC Availability Notice**

Qualified requestors may obtain copies of this report from the Defense Technical Information Center, Cameron Station, Alexandria, Virginia 22314.

### **Disposition Instructions**

Destroy this report when no longer needed. Do not return it to the originator.

SECURITY CLASSIFICATION OF THIS PAGE (When Data Entered)

DD FORM 1 JAN 73 1473

VERSION OF 1 NOV 65 IS OBSOLETE

SECURITY CLASSIFICATION OF THIS PAGE (When Data Entered)

## 20. ABSTRACT (Cont'd)

An ignition-limits apparatus was developed, utilizing an evacuable autoclave at one atmosphere. Measurements made with diesel fuel vapors in air, diluted with various amounts of water vapor, established that such mixtures containing more than about 24 mole% water vapor cannot burn.

Vapor pressure measurements, made in a modification of the same apparatus, confirmed that FRF systems containing 10 vol% water and 6 vol% surfactant are blanketed by equilibrium vapors containing at least 24 mole% water for liquid temperatures greater than about 70°C.

The flash points of diesel fuel FRF blends containing 10 vol% water are about the same as those of the base fuel when its flash point is less than about 70°C. When the base fuel flash point exceeds 70°C, no flash point is detectable for the FRF.

A special apparatus was developed to measure liquid-surface evaporative cooling and liquid-surface heating effects in the vicinity of a simulated flame on the FRF surface. The results confirmed that evaporative cooling effects are significant, but that they are not responsible for the self-extinguishing properties of FRF. In fact, the data indicate that heat transfer effects in front of the simulated flame provide sufficient surface heating to generate greater than the 24 mole% water vapor composition adjacent to the surface needed for self-extinguishment, even when the temperature of bulk liquid FRF is as low as 0°C.

Horizontal flame channel experiments with FRF-type blends containing 6 vol% surfactant indicate that the lowest water content of the liquid which prevents vapor burning in some dynamic situations is 5 vol% or less.

Equilibrium vapor pressure measurements indicate that FRF-type blends containing 6 vol% surfactant and between about 2 and 10 vol% water are micro-emulsions which exert equilibrium water partial pressures significantly less than that of pure water. When the water content is less than about 1 vol%, these systems appear to be micellar solutions with even lower equilibrium water partial pressures.

## FOREWORD

This report was prepared at the U.S. Army Fuels and Lubricants Research Laboratory (AFLRL), Southwest Research Institute, under DoD Contract Nos. DAAK70-80-C-0001 and DAAK70-82-C-0001. The project was administered by the Fuels and Lubricants Division, U.S. Army Mobility Equipment Research and Development Command (MERADCOM), Fort Belvoir, Virginia 22060, with Mr. F.W. Schaekel, DRDME-VF, serving as Contracting Officer's Representative. This report covers the period of performance from 13 May 1980 to 31 December 1982.

DIIB  
COPY  
INSPECTED  
2

Account of Pop	
WILLIAM	<input checked="" type="checkbox"/>
WILLIAM	<input type="checkbox"/>
WILLIAM	<input type="checkbox"/>
Dist Special	

## ACKNOWLEDGEMENTS

Acknowledgement is given to Messrs. J.P. Pierce and R.C. Haufler for conducting laboratory and flammability experiments as well as to Mr. J.W. Pryor and Mrs. D. Kilhorn for editorial assistance in producing this report.

Special acknowledgement is given to Messrs. M.E. LePera, F.W. Schaekel and S.J. Lestz for their participation, encouragement, and suggestions.

## TABLE OF CONTENTS

	<u>Page</u>
I. INTRODUCTION . . . . .	6
II. EXPERIMENTAL . . . . .	9
A. Flammability Limits . . . . .	9
B. Vapor Pressures . . . . .	15
C. Particle Size Measurements. . . . .	23
D. Horizontal Flame Propagation. . . . .	24
E. Flash Point Phenomena . . . . .	25
F. Liquid Surface Heating Phenomena. . . . .	28
III. DISCUSSION . . . . .	36
A. Inter-relationships Among Observed Vapor Pressure, Flammability Limits, Flash Points, and Pool Flame Propagation . . . . .	36
B. Ability of FRF to Burn in Mist Form and On Wicks. . . . .	40
IV. CONCLUSIONS . . . . .	41
V. RECOMMENDATIONS. . . . .	43
VI. LIST OF REFERENCES . . . . .	44
APPENDIX-FUEL PROPERTIES . . . . .	47
LIST OF ABBREVIATIONS AND ACRONYMS . . . . .	51

## LIST OF TABLES

<u>Table</u>	<u>Page</u>
1 Experimental Water Vapor Partial Pressures Over Aqueous Diesel Fuel Blends With 84/6 Fuel/Surfactant Volume Ratio . .	17
2 Experimental Water Vapor Partial Pressures Over Aqueous Diesel Fuel Blends With Various Fuel/Surfactant Ratios. . . .	17
3 Apparent Diameters of Microemulsion Droplets . . . . .	24
4 Summary of Flame Channel Pool Burning Data for Water-Containing, Surfactant-Stabilized, 72°C (162°F) Flash Point Diesel Fuel at 77°C (170°F) . . . . .	26
5 Flammability of FRF Blends. . . . .	27
6 Fuel Channel Transient Data . . . . .	33

## LIST OF ILLUSTRATIONS

<u>Figure</u>	<u>Page</u>
1 Basic Research in Support of Fire-Resistant Diesel Fuel Development . . . . .	10
2 Illustration of Flammability Limits Apparatus . . . . .	11
3 Photograph of Flammability Limits Apparatus . . . . .	11
4 Flammability Diagram for Isooctane Vapor . . . . .	13
5 Flammability Diagram for 45°C Flash Point Diesel Fuel Vapor . .	13
6 Flammability Diagram for 60°C Flash Point Diesel Fuel Vapor . .	14
7 Flammability Diagram for 72°C Flash Point Diesel Fuel Vapor . .	14
8 Composite Flammability Diagram for 45°, 60°, and 72°C Flash Point Diesel Fuels . . . . .	15
9 Drawing of Vapor Pressure Cell . . . . .	16
10 Water Vapor Partial Pressure Over Aqueous Diesel Fuel Blends With 84/6 Fuel/Surfactant Volume Ratio . . . . .	19
11 Water Vapor Partial Pressure Over Aqueous Diesel Fuel Blends With Various Fuel/Surfactant Ratios at 66°C . . . . .	19
12 Correlated Vapor Liquid Equilibria . . . . .	20
13 Correlation of One-Atmosphere Water-Vapor-Content With Liquid Surface Temperature . . . . .	20
14 Influence of FRF Water Content on Water Heat of Vaporization Derived from Correlated Vapor Pressure Data . . . . .	21
15 Influence of Water Content on Differential Heat of Solution of Diesel Fuel Micellar Solutions . . . . .	22
16 Vapor Pressure of Neat Diesel Fuel . . . . .	23
17 Illustration of Controlled Temperature Horizontal Flame Propagation Channel . . . . .	25
18 Photograph of Flame-Propagation-Simulator Fuel Channel . . . .	29
19 Annotated Illustration of Flame-Propagation-Simulator Fuel Channel . . . . .	29
20 Dimensional Drawing of Flame-Propagation-Simulator Fuel Channel . . . . .	30
21 Typical Strip Chart Recorder Traces of Liquid Surface Temperature Near Flame Simulator in Fuel Channel. . . . .	31
22 Influence of Neat Diesel Fuel Initial Temperature on Surface Heating Rate Adjacent to Flame Simulator . . . . .	34



LIST OF ILLUSTRATIONS  
(Cont'd)

<u>Figure</u>	<u>Page</u>
23 Influence of FRF Initial Temperature on Surface Heating Rate Adjacent to Flame Simulator . . . . .	34
24 Influence of Neat Fuel Initial Temperature on Steady-State Surface Temperature Adjacent to Flame Simulator . . . . .	35
25 Influence of FRF Initial Temperature on Steady-State Surface Temperature Adjacent to Flame Simulator . . . . .	35
26 Influence of Initial Water Content of Aqueous Diesel Fuel Blends on Surface Heating Rate Adjacent to Flame Simulator . .	36
27 Equilibrium Vapor Composition and Flammability Properties versus FRF Water Content . . . . .	37
28 Equilibrium Flammability Diagram for FRF-Type Fuel-Water Blends at One-Atmosphere . . . . .	39
29 Qualitative Illustration of Transition from Nonflammable-to- Flammable Vapors After Total Vaporization from a Wick or of Mist Droplets . . . . .	41

## I. INTRODUCTION

Fire-resistant fuel for ground vehicles has been a continuing need for the U.S. armed forces and the transportation industry. Such fuel would reduce the threat of fire to vehicles as well as to personnel. Accordingly, various means have been investigated for reducing fuel fire vulnerability of Army combat vehicles by altering fuel compositions. Extensive laboratory studies have yielded clear-to-hazy fire-resistant fuel (FRF) surfactant-stabilized microemulsions\* of water in diesel fuel. (1,2)\*\* The surfactant is a mixture of reaction products of diethanolamine and oleic acid. Flammability and ballistic tests reveal diminished mist flammability, and such tests demonstrate rapid self-extinguishment of pool fires, even at temperatures above the base fuel flash point. The diminished mist flammability can be explained, at least in part, in terms of reduced atomization stemming from viscosity increases of 50 percent or more normally observed with FRF. However, because of their high atomization pressures, unmodified diesel engines experience no difficulties in starting, idling, and running on such fuels under typical operating conditions.

The mechanisms by which water (or liquid halons) mitigate liquid hydrocarbon flammability hazards have not been fully identified experimentally. However, results of flammability and engine experiments conducted in this laboratory with diesel fuel containing 5 liq. vol% bromochloromethane suggested the dominance of physical mechanisms in rendering the bulk liquid nonflammable in such systems.(3)

There are various mechanisms by which the presence of water may lead to self-extinguishment of burning pools of these aqueous microemulsions. Based upon well established principles of chemistry and physics, it is apparent that various combinations and extents of the mechanisms could be operative, depending upon the properties of the base fuel and surfactant. These are as follows:

---

\*Differences between microemulsions and macroemulsions are described in the "Discussion" section of this report.

\*\*Underscored numbers in parentheses refer to the list of references at the end of this report.

- "Phase-rule" maximum liquid surface temperature restriction stemming from presence of coexisting immiscible water and base fuel phases.
- Evaporative cooling of liquid surfaces stemming from high volatility and heat of vaporization of water relative to those of base fuels.
- Liquid surface blanketing with water vapor leading to:
  - reduced reaction rates and flame temperatures stemming from inert-gas dilution effects.
  - energy sink effects stemming from high specific heat of water vapor relative to air.
  - free-radical flame chemistry effects stemming from presence of excess water in unburned gases adjacent to liquid surfaces.

As mentioned previously, experimental observations in this laboratory strongly suggest that the fire resistance of pools of water-containing diesel fuels stems predominantly from physical mechanisms. For example, if chemical mechanisms were important, the ignition and combustion of water-containing fuels in diesel engines would be seriously impaired, and such is not the case. Moreover, the autoignition temperature (ASTM E 659) of surfactant-containing diesel fuel is not altered by the addition of up to 10 vol% water. Therefore, the chemical mechanism listed last among the above mechanisms is not considered likely to be important in the case of fire-resistant aqueous diesel fuel emulsions. It is listed only for the sake of completeness.

Recognizing that the flammability mitigation exhibited by pools of fire-resistant diesel fuels stems predominantly from physical mechanisms, it is important to establish which of the listed mechanisms, or combinations thereof, are dominant. The "phase rule" maximum surface-temperature restriction for immiscible systems has been proposed as the "essential" mechanism(4) of the observed fire resistance. This could well be true for aqueous emulsions of hydrocarbon liquids which exhibit flash points (lean limit temperatures) that are significantly higher than 100°C. In such

cases, the maximum liquid surface temperature of 100°C could not generate flammable fuel/air mixtures. On the other hand, in the case of fire-resistant diesel fuels, the flash points of the base fuels are always less than 100°C. Consequently, this physical mechanism would not be expected to contribute to the fire resistance of such fuels, and this has been verified experimentally as part of this study.

The relative importance of evaporative cooling and water vapor blanketing mechanisms cannot be inferred from existing published information.<sup>(5)</sup> Therefore, this basic study has been conducted to develop an improved understanding of the mechanisms by which aqueous diesel fuel emulsions exhibit self-extinguishing properties in the pool-burning mode and the influences of fuel variables thereon. After such information has been established, it should be possible to develop more nearly optimum emulsion formulations.

## II. EXPERIMENTAL

The experimental research has proceeded along two distinct avenues as illustrated in Figure 1. One of these has developed data for correlating measured FRF vapor compositions with (1) experimental flammability limits, (2) observed horizontal flame propagation data, and (3) flash point phenomena. The other has provided data indicating the influence of liquid fuel temperature on (1) surface heating rates and (2) steady-state surface temperatures adjacent to a simulated, surface flame. Both have involved development or adaptation of appropriate laboratory equipment and procedures.

### A. Flammability Limits

The first area selected for study was the dilution effect of water vapor in suppressing the flammability of combustible fuel/air mixtures. Other studies have shown that methane/air mixtures containing water vapor have reduced flammability and flame speed. While such data are available on the effect of water vapor in some of the low-molecular weight hydrocarbon/air mixtures, no data are available on the heavier hydrocarbons common to middle distillate fuels.

An experimental apparatus was assembled to measure the effect of water vapor dilution on the flammability of hydrocarbon-air mixtures. Briefly, the apparatus, which is illustrated in Figures 2 and 3, consists of a heated bomb equipped with transducers and thermocouples to measure static pressure and temperature, respectively. Vacuum generation is provided for pump-down to dispose of gases from previous experiments; for induction of water and fuel vapors from separately controlled, heated, liquid-filled reservoirs; and for induction of conditioned air to achieve the desired total pressure for each experiment. The tube which brings the reactants into the bomb is designed to create swirl to assure adequate mixing. Fuel and water are admitted to the bomb as gases through heated lines, and concentrations are determined by measuring the partial pressure of each component as it is added. The entire system is kept at a constant temperature of approximately 90°C to prevent condensation of fuel or water vapors. A high-voltage spark provides an overwhelming ignition source within the bomb, and flame propagation is detected by a pressure rise in the system.

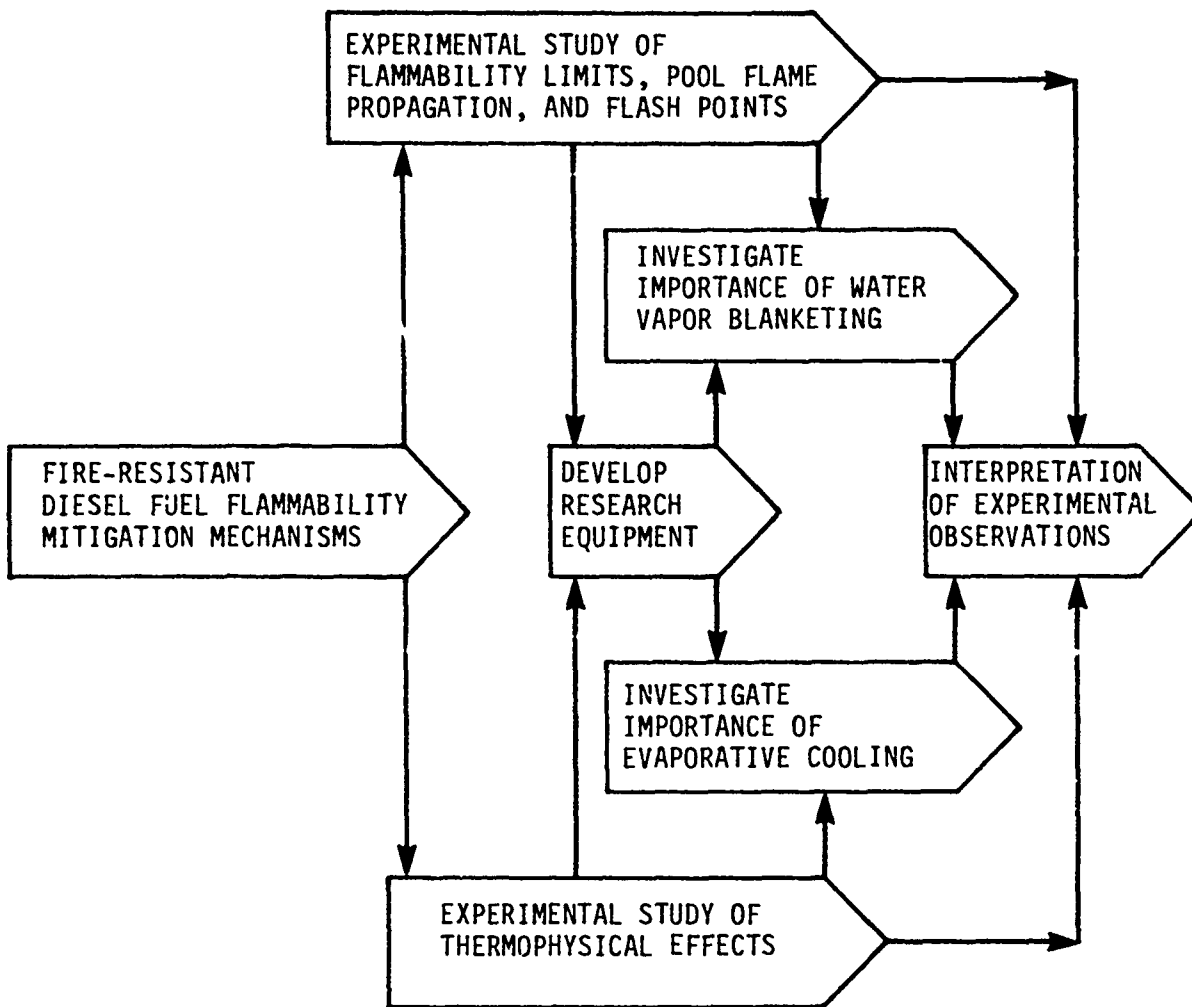


FIGURE 1. BASIC RESEARCH IN SUPPORT OF FIRE-RESISTANT DIESEL FUEL DEVELOPMENT

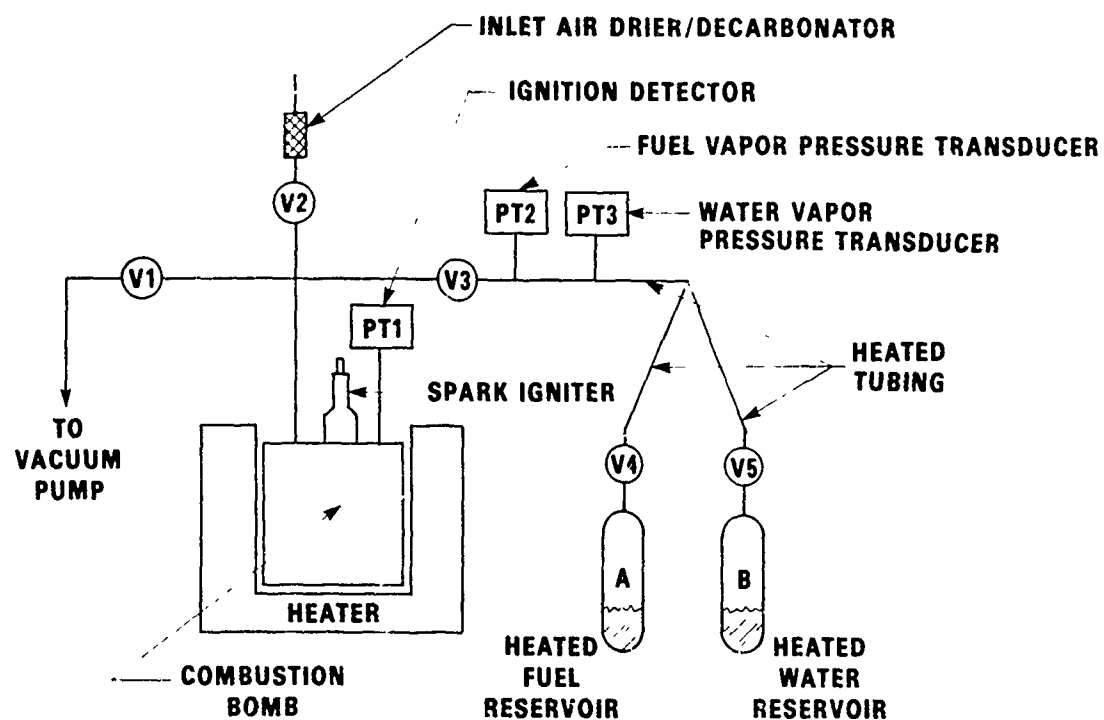


FIGURE 2. ILLUSTRATION OF FLAMMABILITY LIMITS APPARATUS



FIGURE 3. PHOTOGRAPH OF FLAMMABILITY LIMITS APPARATUS

The flammability measurements were performed at atmospheric pressure, so immediately prior to ignition, the air inlet tube was opened. A pressure rise in the bomb was accompanied by an abrupt issuance of gas from the air inlet tube. This was detected by placing a very small metal foil cup over the vertically oriented air inlet tube. The most minute gas flow from the bomb would tip the cup and indicate flame propagation. This air inlet tube was a capillary with an ID of about one millimeter so there was no possibility of the composition changing in the bomb in the short time (~2 sec) that it was open before ignition. This method of detecting pressure rise was much more sensitive than a transducer would have been which could cover the wide range of pressure rises encountered in these experiments.

For low-boiling hydrocarbon fractions, the heated fuel reservoir can be used to supply to the bomb a vapor mixture which has been equilibrated at pre-selected conditions of temperature and vapor-liquid ratio. However, in the case of the diesel fuels of interest to this study, it proved difficult to generate sufficient vapors to achieve the desired fuel partial pressures in the bomb. Consequently, as an alternative approach, 1 vol% of each of the three different diesel fuels to be studied was distilled at zero reflux to yield a totally vaporizable fraction for use in the flammability limits apparatus. Analyses of these fractions and of vapors evolved from the total fuels at the flash point temperature indicate that composition differences among the 1 percent fractions are representative of flash point vapor composition differences. These three base fuels, Nos. 9295, 7225, and 8821, displayed flash points of 45°, 60°, and 72°C, respectively.

The flammability limits apparatus was calibrated with isooctane. A flammability limits diagram for the isooctane vapor/water vapor/air system was determined, and this is presented as Figure 4. The results are in reasonable agreement with literature values (6) for the rich and lean limits of neat isooctane. No literature data on isooctane/air/water vapor could be found. Results of flammability measurements on the diesel fuel vapor/water vapor/air mixtures are presented in Figures 5, 6 and 7. The peak of the flammability diagram, i.e., the water vapor content at which the lean and rich flammability limits converge, occurs in the range of 2 to 2.5 mole percent fuel vapor and 23 to 24 mole percent water vapor, which is similar to that observed for the isooctane calibration fuel.



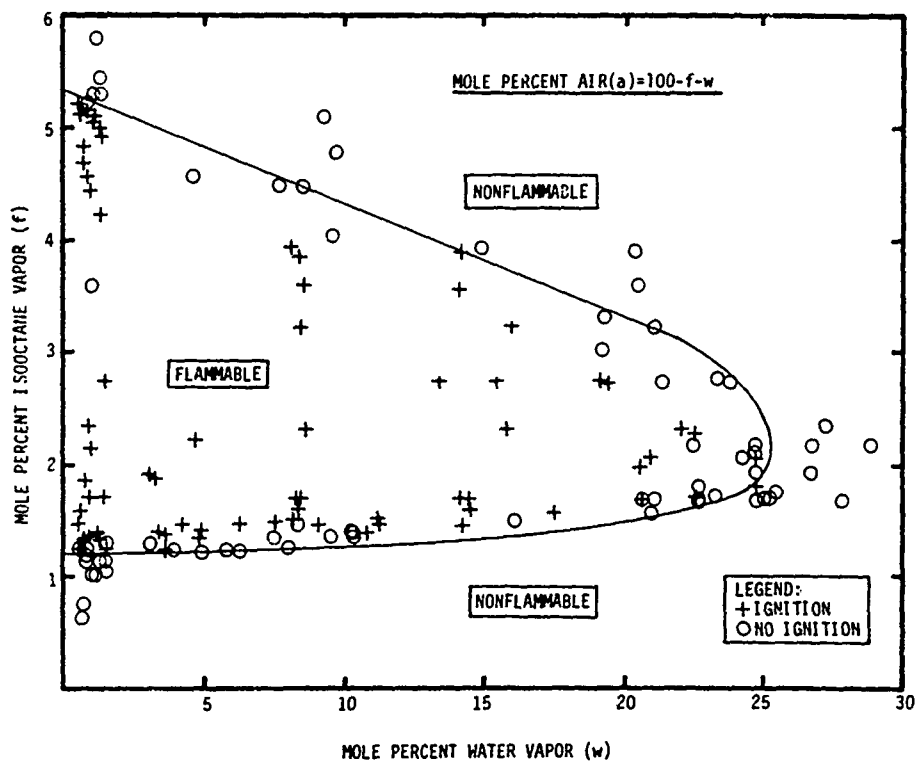


FIGURE 4. FLAMMABILITY DIAGRAM FOR ISOCTANE VAPOR

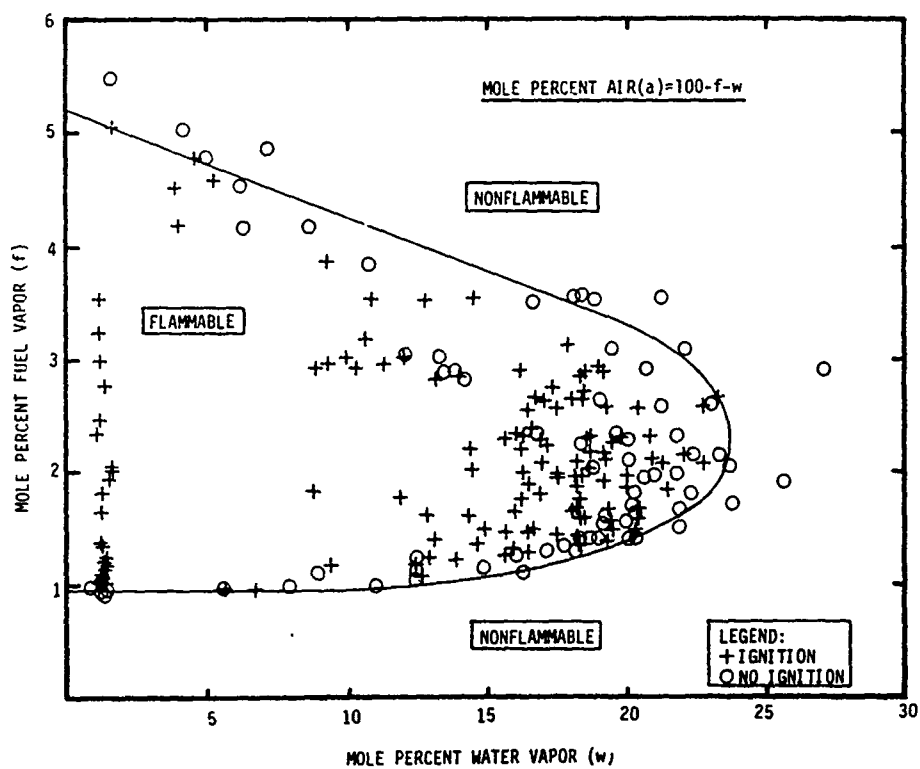


FIGURE 5. FLAMMABILITY DIAGRAM FOR 45°C FLASH POINT DIESEL FUEL VAPOR

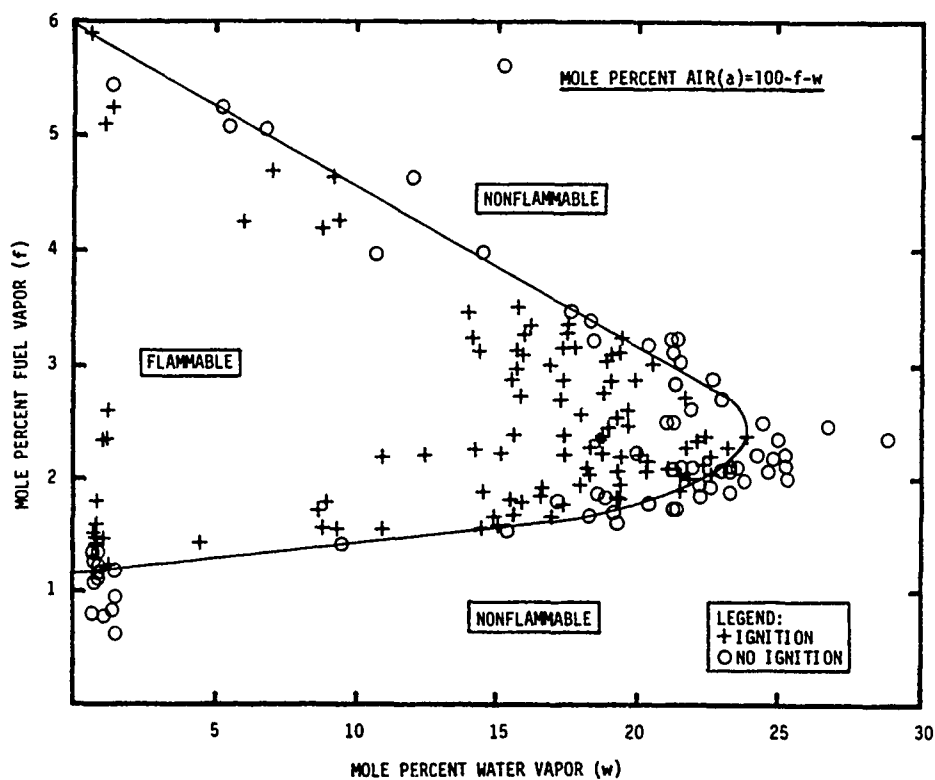


FIGURE 6. FLAMMABILITY DIAGRAM FOR 60°C FLASH POINT DIESEL FUEL VAPOR

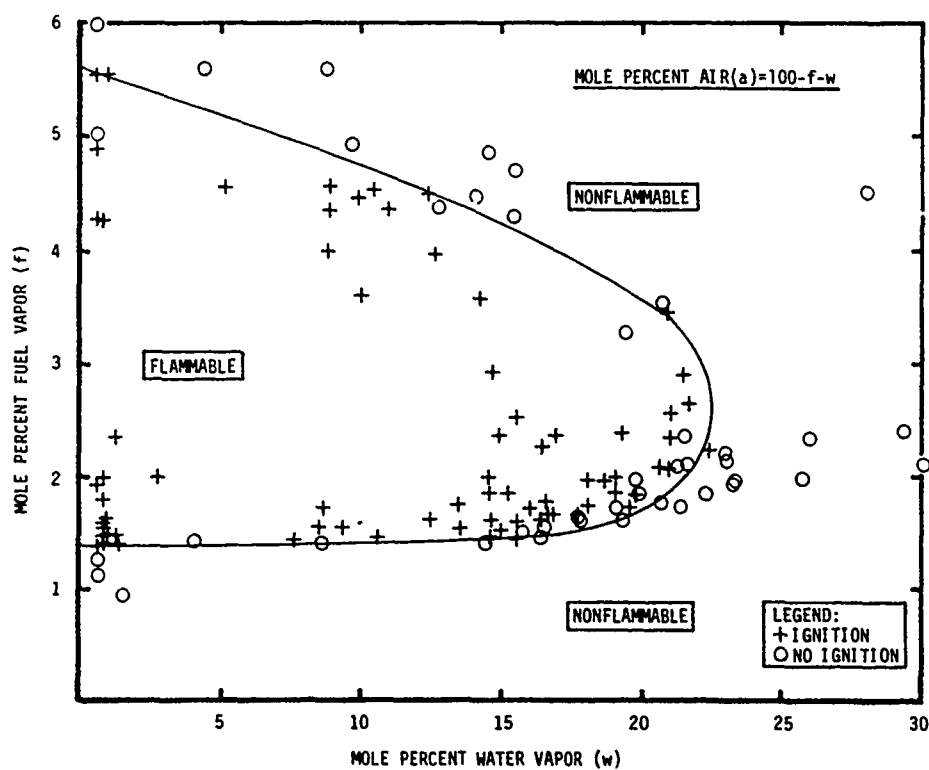


FIGURE 7. FLAMMABILITY DIAGRAM FOR 72°C FLASH POINT DIESEL FUEL VAPOR

The data for the 45°, 60°, and 72°C flash point diesel fuels (Figures 5, 6, and 7) are presented as a composite flammability limits diagram in Figure 8. As in the case of Figures 5, 6, and 7, the flammable region envelope is drawn to include all ignitions, and, as a result, it also includes some non-ignitions. Based on this composite diagram, diesel fuel vapors containing more than about 24 mole percent water vapor should be nonflammable.

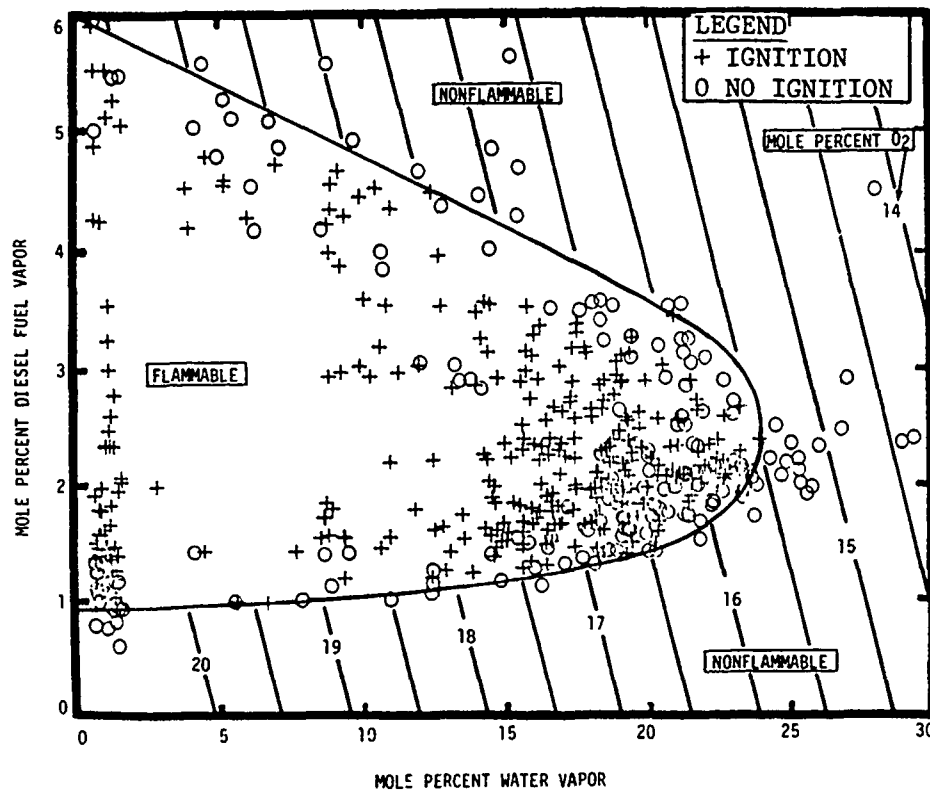


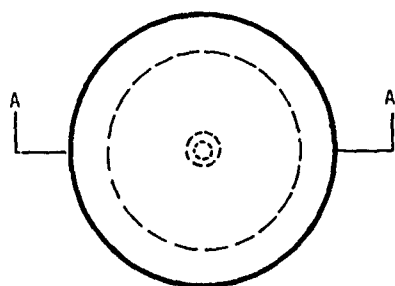
FIGURE 8. COMPOSITE FLAMMABILITY DIAGRAM FOR 45°, 60°, AND 72°C FLASH POINT DIESEL FUELS

#### B. Vapor Pressures

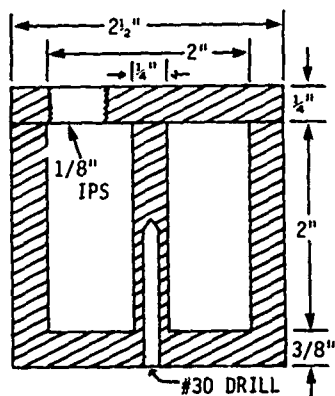
At the completion of the foregoing experiments, a portion of the apparatus for measuring flammability limits was modified to accommodate the measurement of vapor pressure. The purpose was to determine if water-in-fuel microemulsions are truly immiscible systems. Earlier work conducted elsewhere for the Army Research Office (ARO)(4) indicated that water-in-fuel macroemulsions were immiscible systems, i.e., the vapor pressure of water

above the macroemulsion was about the same as that of pure water and did not depend on the concentration of water in the emulsion. However, for the present work, it was recognized that the vapor pressure of water could be concentration dependent in microemulsions.

The apparatus modification comprised replacing one of the heated reservoirs shown in Figure 2 with an aluminum cell designed for precise temperature control (in a regulated bath) and measurement (Figure 9). The fuel sample in this container is frozen with a dry ice/acetone bath, and it is then pumped down, thawed, and pumped down again, successively, until the residual pressure is well below  $10^{-4}$  atm, thereby removing all noncondensable gases



TOP VIEW



SECTION A-A

FIGURE 9. DRAWING OF VAPOR PRESSURE CELL

from the fuel sample. The vapor pressure is then measured directly with the appropriate pressure transducer in the apparatus illustrated in Figure 2 as the deaerated fuel in the aluminum block is allowed to equilibrate at various temperatures, ranging from  $1^{\circ}$  to  $100^{\circ}\text{C}$ .

Vapor pressure measurements were made at  $32^{\circ}$ ,  $49^{\circ}$ ,  $66^{\circ}$  and  $77^{\circ}\text{C}$  on neat diesel fuel and blends containing 2 to 13 vol% surfactant and 0.04 to 16 vol% water. Measurements made on pure water were consistent with vapor pressure tabulations in the literature and showed that the apparatus could yield accurate data. Off-gassing during experiments with diesel fuel containing 6 vol% surfactant indicated the presence of dissolved water in the neat surfac-

tant. This was subsequently confirmed and accounted for by chemical analysis. Temperature control of the system proved to be the most critical factor in achieving repeatability. The results of the measurements made on the

various water/fuel blends are presented in Tables 1 and 2 and Figures 10 and 11.

TABLE 1. EXPERIMENTAL WATER VAPOR PARTIAL PRESSURES OVER AQUEOUS DIESEL FUEL BLENDS WITH 84/6 FUEL/SURFACTANT VOLUME RATIO

Vol% Water	Moles Water per Mole Surfactant*	Vapor Pressure, atm				Relative Vapor Pressure, p/p°			
		32°C	49°C	66°C	77°C	32°C	49°C	66°C	77°C
0.07	0.17	--	--	--	0.033	--	--	--	0.085
0.20	0.49	0.0016	0.016	0.039	0.090	0.035	0.141	0.161	0.23
0.49	1.25	0.013	0.038	0.094	0.165	0.28	0.34	0.39	0.42
0.62	1.58	0.016	0.048	0.118	0.187	0.34	0.43	0.49	0.48
1.13	2.9	0.025	0.063	0.147	0.244	0.55	0.57	0.61	0.62
2.5	6.6	0.028	0.082	0.179	0.321	0.62	0.75	0.74	0.82
4.7	12.4	0.033	0.083	0.196	0.315	0.72	0.75	0.81	0.81
8.8	24.4	0.031	0.089	0.199	0.341	0.66	0.81	0.82	0.87
100.0	∞	0.046	0.110	0.242	0.391	1.00	1.00	1.00	1.00

\*Surfactant molecular weight: 301 g mol/g

TABLE 2. EXPERIMENTAL WATER VAPOR PARTIAL PRESSURES OVER AQUEOUS DIESEL FUEL BLENDS WITH VARIOUS FUEL/SURFACTANT RATIOS

Vol % Water	Vol % Surfactant	Moles Water Per Mole Surfactant	Water Vapor Pressure at 66°C	
			Absolute, atm	Relative to Pure Water, p/p°
0.036	2.2	0.27	0.007	0.029
0.088	2.2	0.67	0.035	0.145
0.152	2.2	1.16	0.073	0.30
0.188	2.2	1.43	0.102	0.42
0.39	2.2	3.0	0.141	0.58
0.78	2.2	6.0	0.173	0.71
1.65	2.2	12.7	0.189	0.78
3.3	2.2	25.8	0.194	0.80
0.067	6.7	0.17	0.000	0.000
0.196	6.7	0.49	0.039	0.161
0.49	6.6	1.25	0.094	0.39
0.62	6.6	1.58	0.118	0.49
1.13	6.6	2.9	0.147	0.61
2.5	6.5	6.6	0.179	0.74
4.7	6.4	12.4	0.196	0.81
8.8	6.1	24.4	0.199	0.82
0.104	13.3	0.13	0.005	0.021
0.37	13.3	0.46	0.042	0.174
0.74	13.2	0.94	0.087	0.36
1.13	13.2	1.45	0.117	0.48
1.70	13.1	2.2	0.146	0.60
4.6	12.7	6.2	0.174	0.72
8.6	12.2	10.9	0.191	0.79
16.1	11.2	24.5	0.190	0.79

In Figure 10, the equilibrium partial pressure of water is correlated with the water content of the liquid at various temperatures. These data show at least two regimes of differing phase behavior as the water content of a fuel/surfactant solution is varied. The results suggest a transition from micellar solutions\*, at low water contents, to microemulsions\*, at higher water contents. The water content at the intersection of the linear correlations varies from about 1 to 2 vol% as the temperature is increased from 32° to 77°C.

The data on effects of surfactant concentration at 66°C are correlated in terms of water partial pressure and water content in Figure 11. The data for the three surfactant-content levels could be brought closer together by correlating them in terms of water/surfactant volume ratio or mole ratio, but they would not be superimposed by such manipulations.

When the correlated lines of Figure 10 are transposed into relative pressures (i.e., the partial pressure of water divided by its absolute vapor pressure), the low-water-content lines converge when extrapolated to the vapor pressure of water at about 6 vol% water in the fuel/water/surfactant liquid, as illustrated in Figure 12. Similarly, the transposed correlated lines for the concentration range above 1-2 liq vol% water converge when extrapolated to the vapor pressure of water at 100 percent water in the liquid.

The correlated vapor pressure data of Figure 10 also are cross-plotted in Figure 13, expressed as equilibrium, one-atmosphere vapor compositions versus liquid temperature, for constant liquid water contents. Based on this correlation, the temperature at which the equilibrium vapor over FRF is 24 mole percent water is about 69°C. This corresponds to the tip of the flammability envelope of Figure 8.

The smoothed water vapor pressure data of Figure 10 were cross-plotted as the logarithm of vapor pressure versus the reciprocal absolute temperature to derive the Clausius-Clapeyron heat of vaporization. The results of this

---

\*Differences between micellar solutions and microemulsions are described in the "Discussion" section of this report.

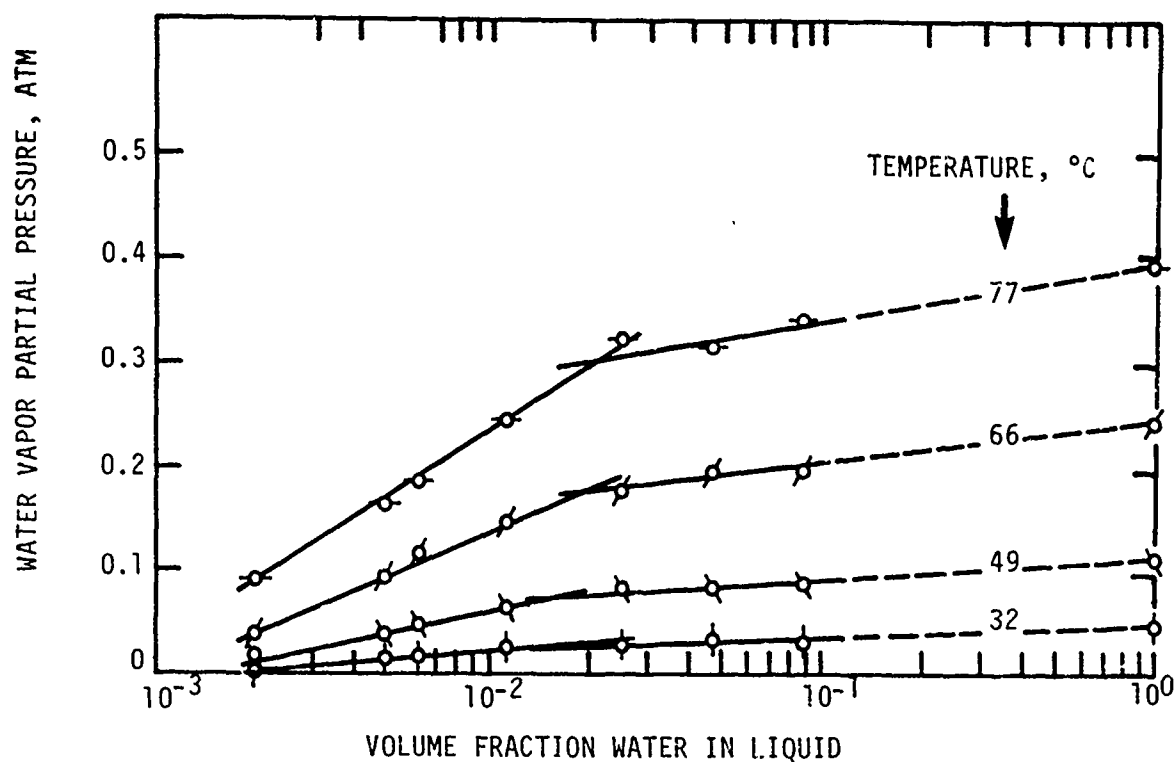


FIGURE 10. WATER VAPOR PARTIAL PRESSURE OVER AQUEOUS DIESEL FUEL BLENDS WITH 84/6 FUEL/SURFACTANT VOLUME RATIO

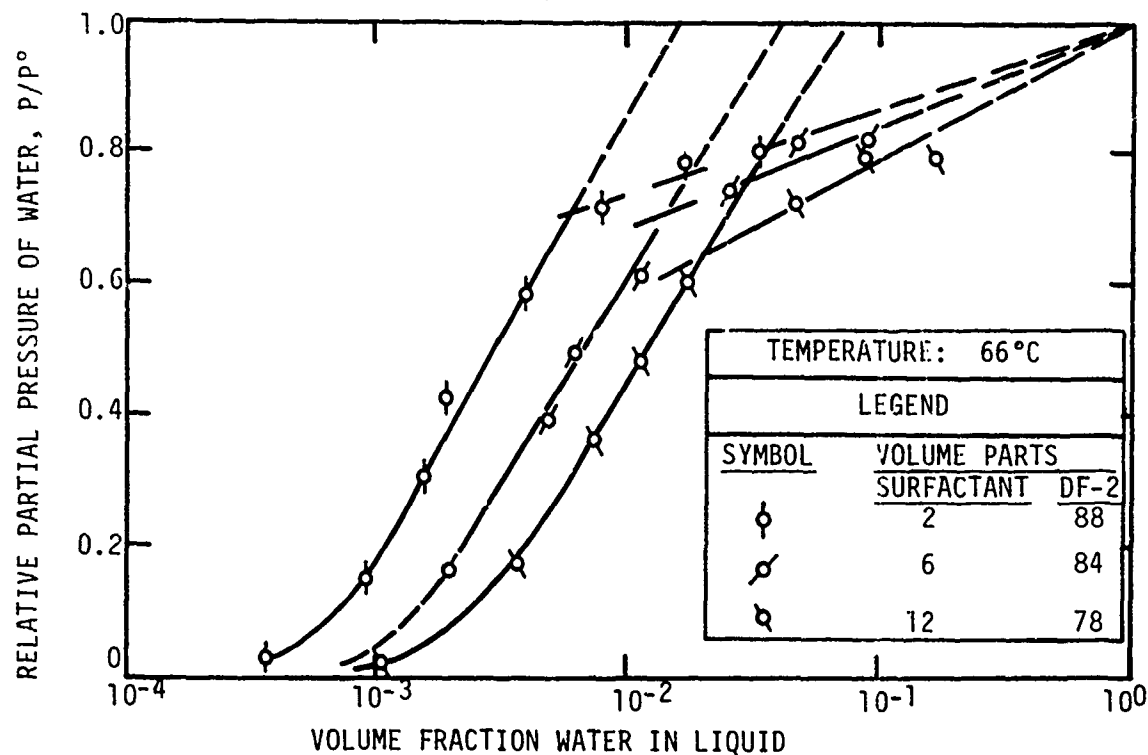


FIGURE 11. WATER VAPOR PARTIAL PRESSURE OVER AQUEOUS DIESEL FUEL BLENDS WITH VARIOUS FUEL/SURFACTANT RATIOS AT 66 °C

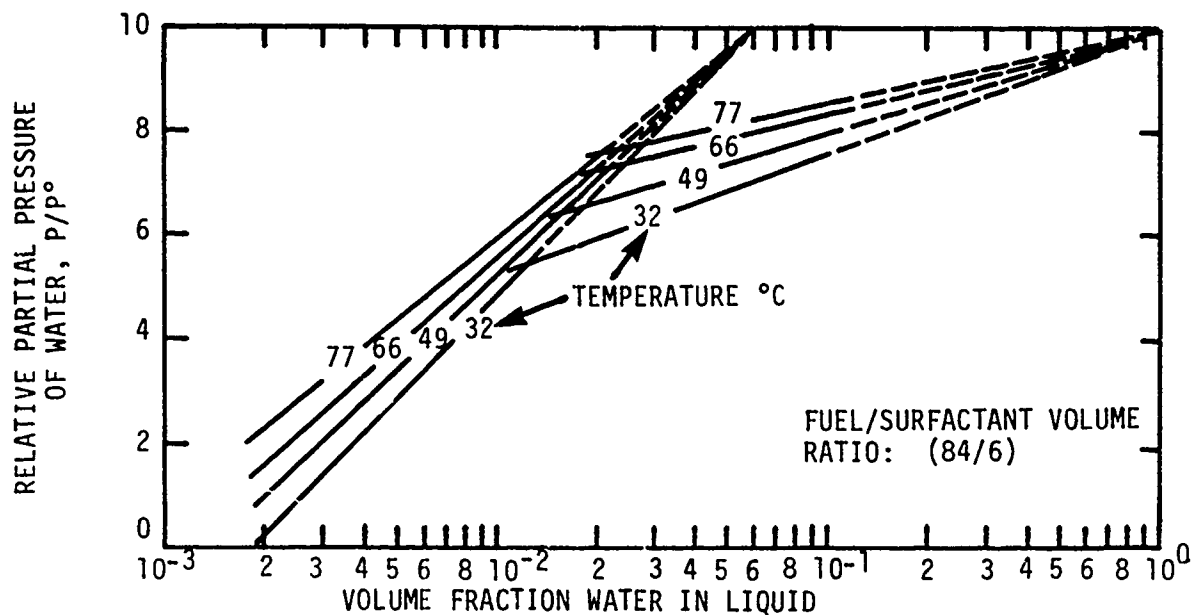


FIGURE 12. CORRELATED VAPOR LIQUID EQUILIBRIA

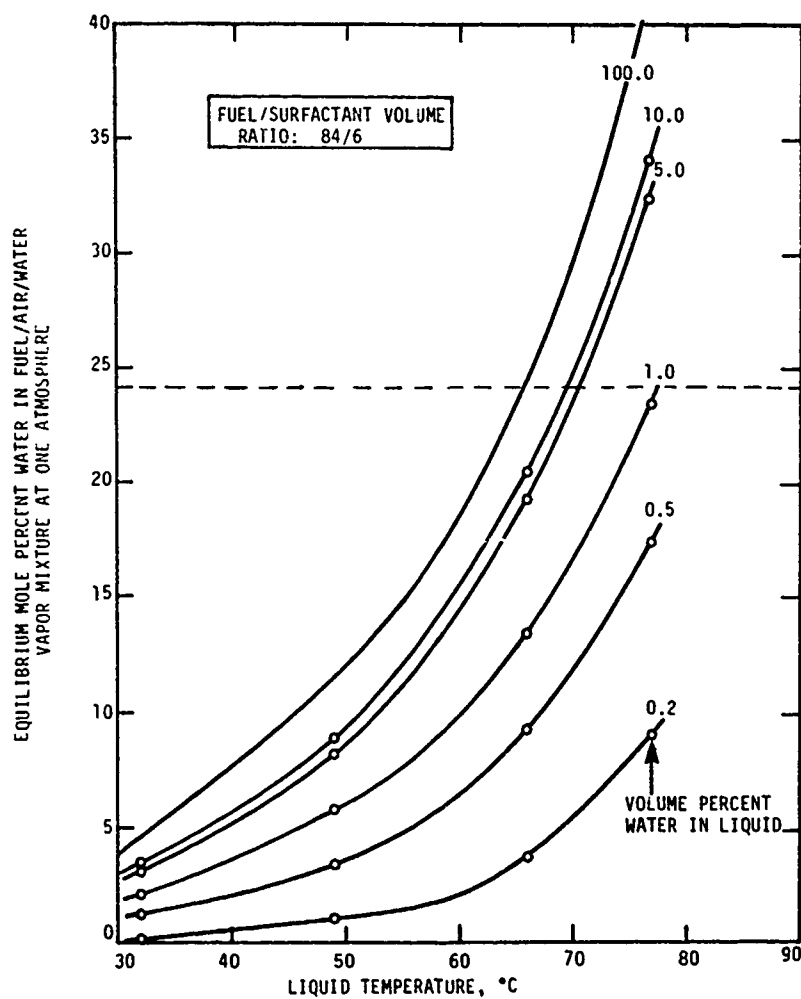


FIGURE 13. CORRELATION OF ONE-ATMOSPHERE WATER-VAPOR-CONTENT WITH LIQUID SURFACE TEMPERATURE



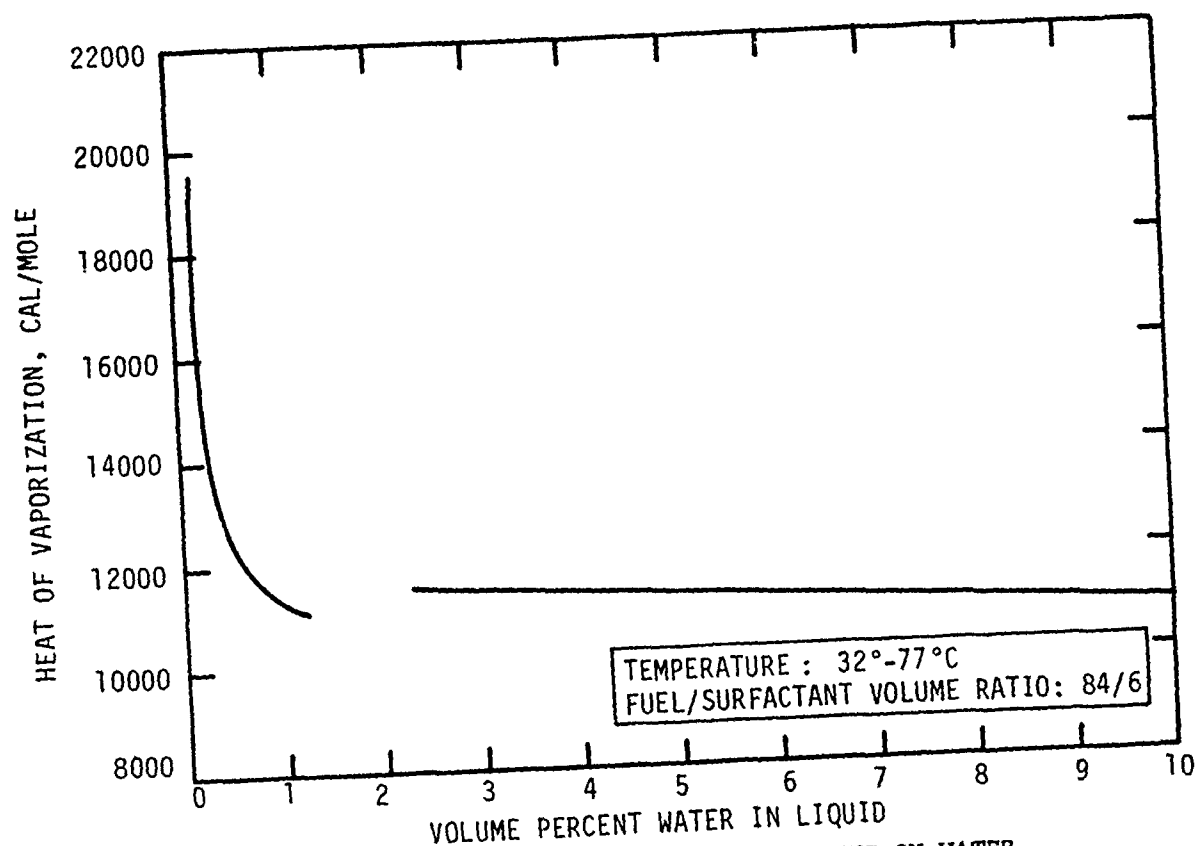


FIGURE 14. INFLUENCE OF FRF WATER CONTENT ON WATER HEAT OF VAPORIZATION DERIVED FROM CORRELATED VAPOR PRESSURE DATA

plot which are presented in Figure 14 indicate a discontinuous relationship in the transition region between about 1 and 2 vol% water in the liquid. This may be an artifact of the data smoothing, or it may reflect the differences between micellar solution molecular processes and microemulsification phenomena. A Clausius-Clapeyron plot was also derived from the relative vapor pressure,  $p/p_0$ , correlation of Figure 12, using the curves for less than 2 vol% water. In this case, the slopes yield the difference between the heats of vaporization of water from the micellar solution and from pure water. The resulting "differential heats of solution" are portrayed in Figure 15.

The foregoing results for systems containing 84/6 vol/vol ratio of fuel to surfactant indicate that in the microemulsion composition range, >2 vol% water, the water heat of vaporization is only slightly greater than that calculated for pure water. On the other hand, as the water content is

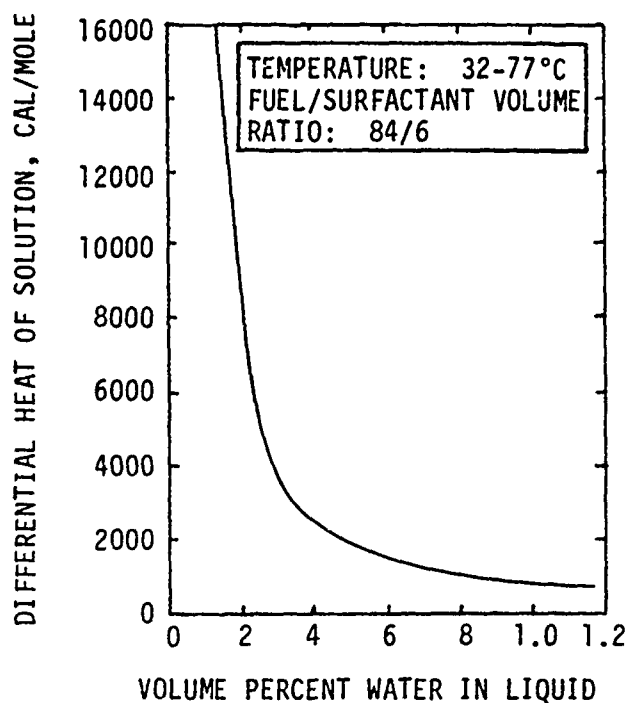


FIGURE 15. INFLUENCE OF WATER CONTENT ON "DIFFERENTIAL HEAT OF SOLUTION" OF DIESEL FUEL MICELLAR SOLUTIONS

decreased below about 1 vol%, the derived "heat of solution" increases rapidly, evidently reflecting the importance of hydrogen bonding in micelle formation. This further strengthens the premise expressed earlier that the transition in vapor pressure trends observed in the 1 to 2 vol% water range is the boundary between micellar solutions and microemulsions.

The vapor pressure curve measured for the neat DF-2 base fuel used in the foregoing FRF-type blends is presented in Figure 16. These results reveal substantially higher vapor pressures for the neat fuel than would be encountered in actual practice. These data suggest a flash point of  $\sim 30^{\circ}\text{C}$  whereas the actual measured flash point was  $72^{\circ}\text{C}$ . It appeared that the fuel sample contained trace volatile ingredients which would be lost rapidly upon open exposure to normal ambient or higher temperatures such as in a flash point apparatus. The volatiles were not excluded in the previously-described vapor pressure apparatus because the sample was maintained at cryogenic temperatures when it was exposed to a vacuum. Accordingly, the correlation of Figure 16 has been presented only for the sake of completeness, but it is not considered representative of the volatility under realistic exposure conditions.

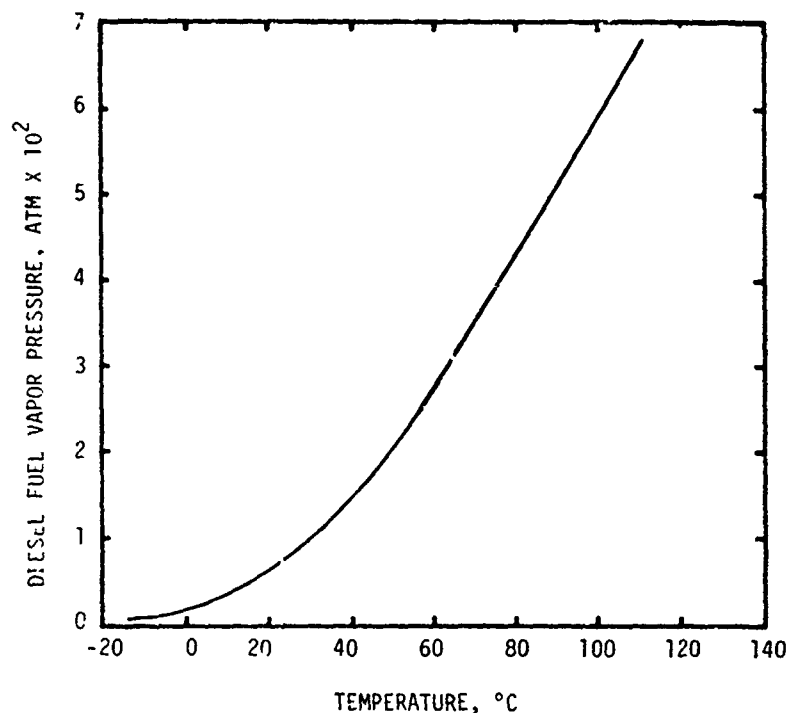


FIGURE 16. VAPOR PRESSURE OF NEAT DIESEL FUEL

#### C. Particle Size Measurements

In order to develop additional information on the effects of water content on FRF-type blends, two of the samples used for vapor pressure measurements were also subjected to droplet size measurements by photon correlation spectroscopy (PCS). Each of the samples exhibited strong Rayleigh scattering. In this technique, a vertically polarized laser beam is scattered by the suspension of droplets.

A special photomultiplier detects single photons scattered in the horizontal plane at a given angle from the incident beam. Since the droplets are in random thermal (Brownian) motion, there is a fluctuation in time of the number of scatterers in the scattering volume seen by the detector. In effect, the droplets (particles) are continually diffusing about their equilibrium positions. This concentration fluctuation causes a fluctuation in time of the detected light. By analyzing the intensity fluctuations, the diffusion coefficient of the droplets, which is inversely related to the droplet size, is obtained. Assuming the droplets within each of the emulsion samples to be rigid monodispersed spheres, their solvated or hydrodynamic diameters were calculated, and the results are presented in Table 3.

---

TABLE 3. APPARENT DIAMETERS OF MICROEMULSION DROPLETS

---

<u>Vol % Water*</u>	<u>Moles Water per Mole Surfactant</u>	<u>Apparent Droplet Diameter**, A</u>		
		<u>32°C</u>	<u>49°C</u>	<u>66°C</u>
1.13	2.9	43	--	--
4.7	12.4	241	171	166

\*Samples filtered repeatedly through 0.4  $\mu$ m polycarbonate-type filter.

\*\*Data reduction based on density and refractive index of base fuel at test temperature.

---

These results provide an additional indication that blends containing about 1 vol% water or less are dispersions of swollen micelles (micellar solutions) in contrast with higher water-content blends which contain surfactant-sheathed water droplets (microemulsions)\*.

#### D. Horizontal Flame Propagation

In order to relate the experimental flammability limits and vapor pressure data to the flammability characteristics of FRF, a series of experiments was conducted in a controlled-temperature, horizontal, flame propagation channel. The device, which is illustrated in Figure 17, comprises a test liquid channel 8.5 cm wide, 4 cm deep, and 61 cm long (inside dimensions), open on top. A closed, heat-transfer fluid chamber of identical, but inverted, dimensions forms the base of the channel. In these experiments, the fuel was preheated to 77°C in a closed vessel, while the channel was equilibrated at 77°C. In each experiment, the channel was fully filled with the test fluid, and the illustrated wick was placed in the liquid 15 cm from one end of the channel. The wick was then lighted at one end, and the time required for the flame to depart from the wick (induction period) and the additional

---

\*Differences between micellar solutions and microemulsions are described in the "Discussion" section of this report.

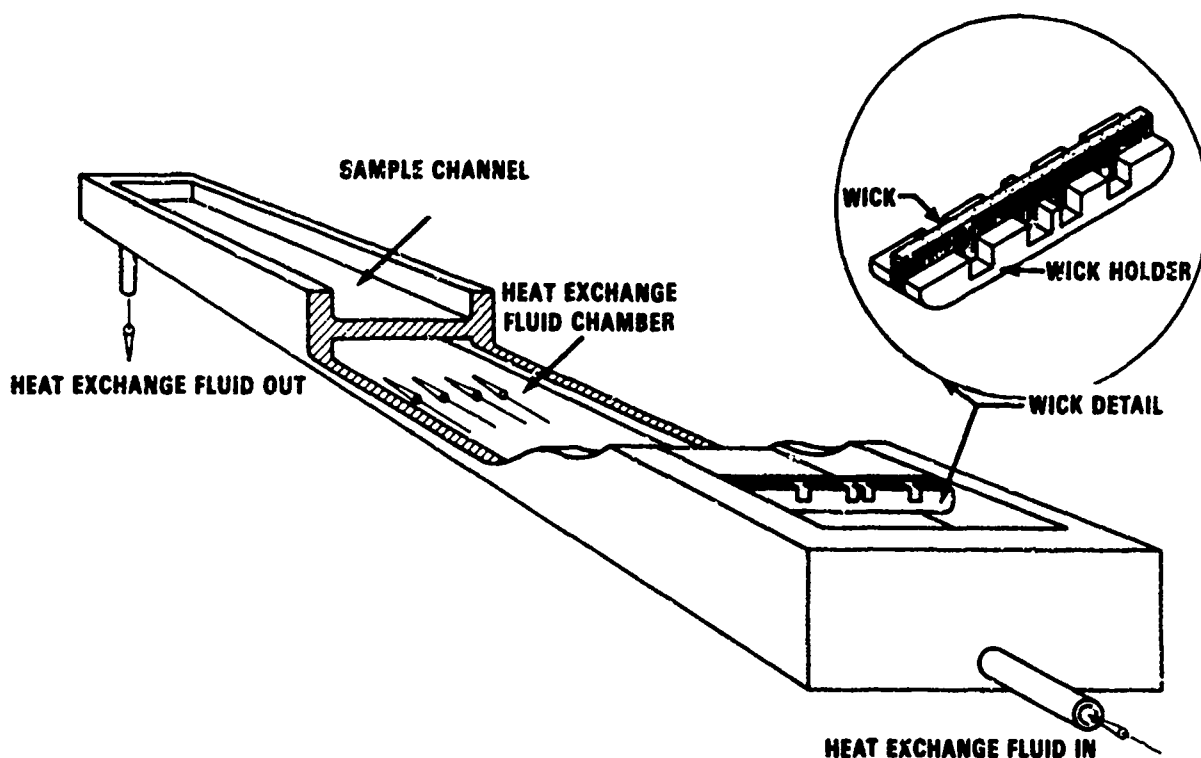


FIGURE 17. ILLUSTRATION OF CONTROLLED-TEMPERATURE HORIZONTAL FLAME PROPAGATION CHANNEL

time required for it to traverse the length of the channel were recorded. Results thus obtained with fuel-plus-surfactant blends containing 10, 5, 1, 0.5, and 0 vol% added water are presented in Table 4 and discussed in a later section of this report.

#### E. Flash Point Phenomena

Apparent flash point anomalies were observed with various batches of FRF made with the same or with different base fuels. These were re-examined by conducting flash point measurements on a series of 10 vol% water, FRF blends

TABLE 4. SUMMARY OF FLAME CHANNEL POOL BURNING DATA FOR  
WATER-CONTAINING, SURFACTANT-STABILIZED, 72°C (162°F) FLASH POINT  
DIESEL FUEL AT 77°C (170°F)

	<u>Induction Period, sec</u>	<u>Channel Traverse Time, sec</u>
Base Fuel (3)*	63 ± 25 (Undulating Wick Flame)	27 ± 3
93.5 vol% Base Fuel, 0.5 vol% Water, and 6 vol% Surfactant (2)*	15 ± 6 (Undulating Wick Flame)	36 ± 2
93.0 vol% Base Fuel, 1.0 vol% Water, and 6 vol% Surfactant (2)*	>1200 (Undulating Wick Flame)	No Ignition of Pool
89 vol% Base Fuel, 5 vol% Water, and 6 vol% Surfactant (1)*	>1200 (Steady Wick Flame)	No Ignition of Pool
84 vol% Base Fuel, 10 vol% Water, and 6 vol% Surfactant FRF (1)*	>1200 (Steady Wick Flame)	No Ignition of Pool

\* Number in parentheses denotes the number of tests.

in which the surfactant content was varied from 1 to 13 vol%, in 1-percent steps, using the reference base fuel, No. 8821. Such measurements were also made on 10 vol% water, FRF blends containing 1, 6, and 10 vol% surfactant, using a lower flash point base fuel, No. 7908. Results of these tests are presented in Table 5 together with flash point data previously obtained with these and other base fuels. Table 5 also includes results of mist flammability evaluations.

The flash point data demonstrate complex results. Flash points were observed with FRF blends prepared from base fuels having flash points of less than 70°C. With FRF blends made from higher flash point base fuels (70°C or greater), the pilot flame was extinguished by the vapors escaping from the apparatus. During the course of these tests, blowout of the pilot flame was observed between 77° and 82°C. Upon further increase of temperature, a

TABLE 5. FLAMMABILITY OF FRF BLENDS

Code No. of DF-2 Base Fuel	Volume %		Pensky Martens Closed Cup Flash Test (1) (ASTM D 93)			Cleveland Open Cup (ASTM D 92)	AFLRL Mist Flashback <sup>(2)</sup>
	Surfactant	Water	Pilot Blowout, °C	Outside Flash, °C	Flash Point, °C	Fire Point, °C	Rating cm
7225	0	0	---	---	60,61	84	22
	1	1	---	---	64	90	---
	3-5	5	---	---	66,66	94	---
	6	10	---	---	60,61,65, 66,67	100,103	17,15
	6	10	77	82	NF	---	---
	10	10	77	82	NF	---	---
	610-16	---	---	---	---	---	---
7908	0	0	---	---	54,54	---	---
	1	10	77	85	NF	---	---
	6	10	---	---	58,58	---	---
	10	10	77	85	NF	---	---
7907	0	0	---	---	63	---	---
	6	10	---	---	NF	---	---
7996	0	0	---	---	68	---	---
	6	10	---	---	NF	---	---
8821	0	0	---	---	70,72	---	---
	1	10	77	93	NF	---	---
	2	10	77	93	NF	---	---
	3	10	77	93	NF	---	---
	4	10	77	88	NF	---	---
	5	10	77	88	NF	---	---
	6	10	77	88	NF	---	---
	7	10	82	91	NF	---	---
	8	10	82	91	NF	---	---
	9	10	82	91	NF	---	---
	10	10	77,77	93,82	NF	---	---
	11	10	77	82	NF	---	---
	12	10	77,77	84,82	NF	---	---
	13	10	77	82	NF	---	---
8445	0	0	---	---	75	---	---
	6	10	---	---	NF	---	---
7931	0	0	---	---	88	---	---
	6	10	---	---	NF	---	---

{1}"NF" means no normal flash point could be observed. All values are the average of at least two tests, including those rated "NF".

(2)Reference 1.

flash was observed (between 82° and 93°C) outside of the cup, near the external relight flame, as the window of the apparatus was opened. Apparently, a flammable mixture formed as vapors escaped from the closed cup and mixed with air. When the liquid temperature in the apparatus reached 100°C, vigorous boiling was observed, at which time the tests were terminated. If a normal flash point was not detectable, the letters "NF" appear in Table 5. It should be noted that in each occurrence of "NF" a duplicate run was

performed to substantiate the results. The flammability mitigation mechanism implications of these results are discussed in a subsequent section of this report.

#### F. Liquid Surface Heating Phenomena

An apparatus was developed for investigating evaporative cooling effects on flame propagation over aqueous diesel fuel microemulsions. The design and operating principles of this apparatus and experimental results obtained with it are described and discussed in the following paragraphs.

The device, which is illustrated in Figures 18, 19, and 20, comprises a test liquid channel 8.5 cm wide, 4 cm deep, and 61 cm long (inside dimensions), open on top. A closed, heat-transfer fluid chamber of identical, but inverted, dimensions forms the base of the channel. Aluminum plates form walls on the sides and one end of the channel, extending 11 cm above the top edges of the test liquid channel. Fast response thermocouples are positioned at the midpoint of the test liquid channel (bulk liquid temperature); just within the liquid surface 6 mm from the midpoint of the outer surface of a horizontal cylindrical electric heater which is half submerged in the liquid surface (liquid surface temperature); and at the midpoint of the heat-transfer fluid chamber (channel temperature).

During an experiment, the channel and test liquid are preheated to several degrees C above the desired test temperature. After the liquid is transferred into the channel (via a long-stem funnel) and becomes quiescent, all temperatures are noted, a strip-chart recorder is started, and the semi-submerged heater (flame simulator) is energized at a preset voltage. After 5-10 minutes, the experiment is terminated and all temperatures noted. As shown in Figure 21, the strip-chart recording of the liquid surface temperature is processed by measuring the linear slope of the trace (fluctuating) of the surface temperature-versus-time to obtain the surface heating rate.

The fluctuations are believed to reflect randomly undulating surface flow "schlieren" stemming from localized variations in heat transfer along the



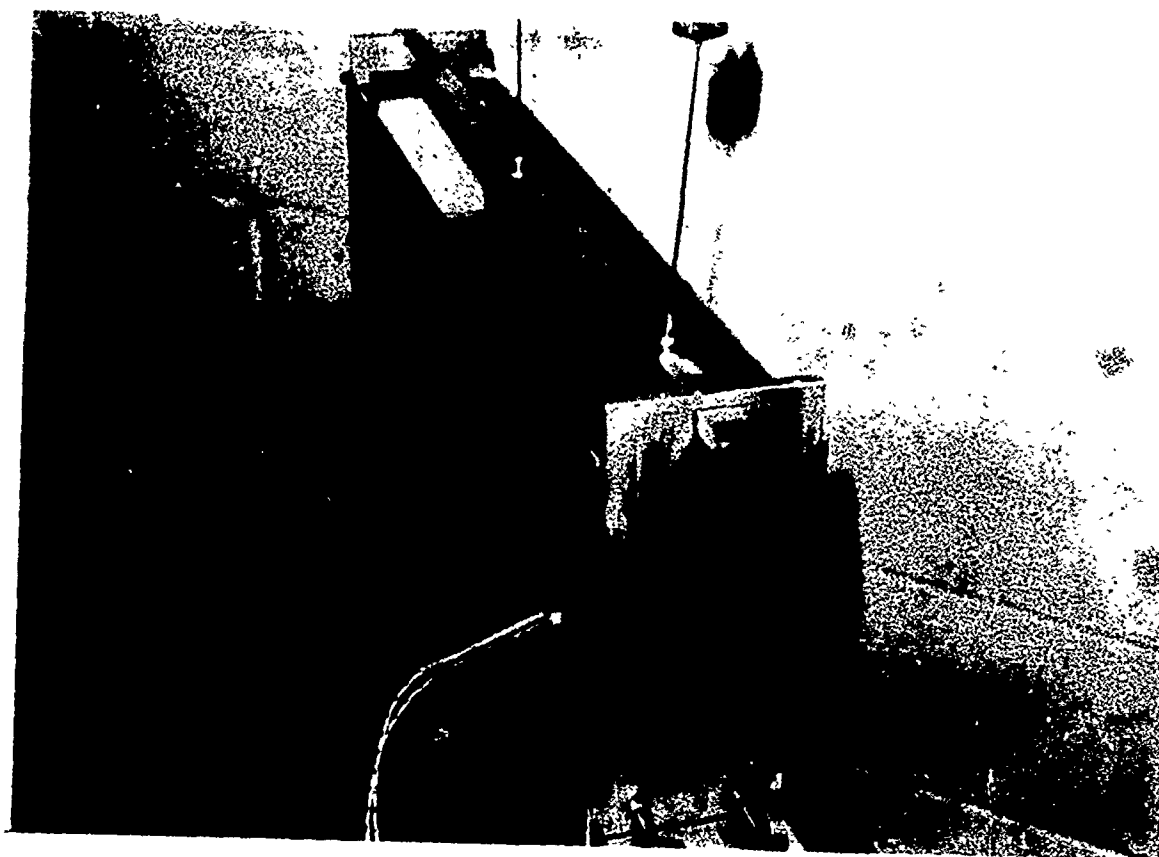


FIGURE 18. PHOTOGRAPH OF FLAME-PROPAGATION-SIMULATOR FUEL CHANNEL

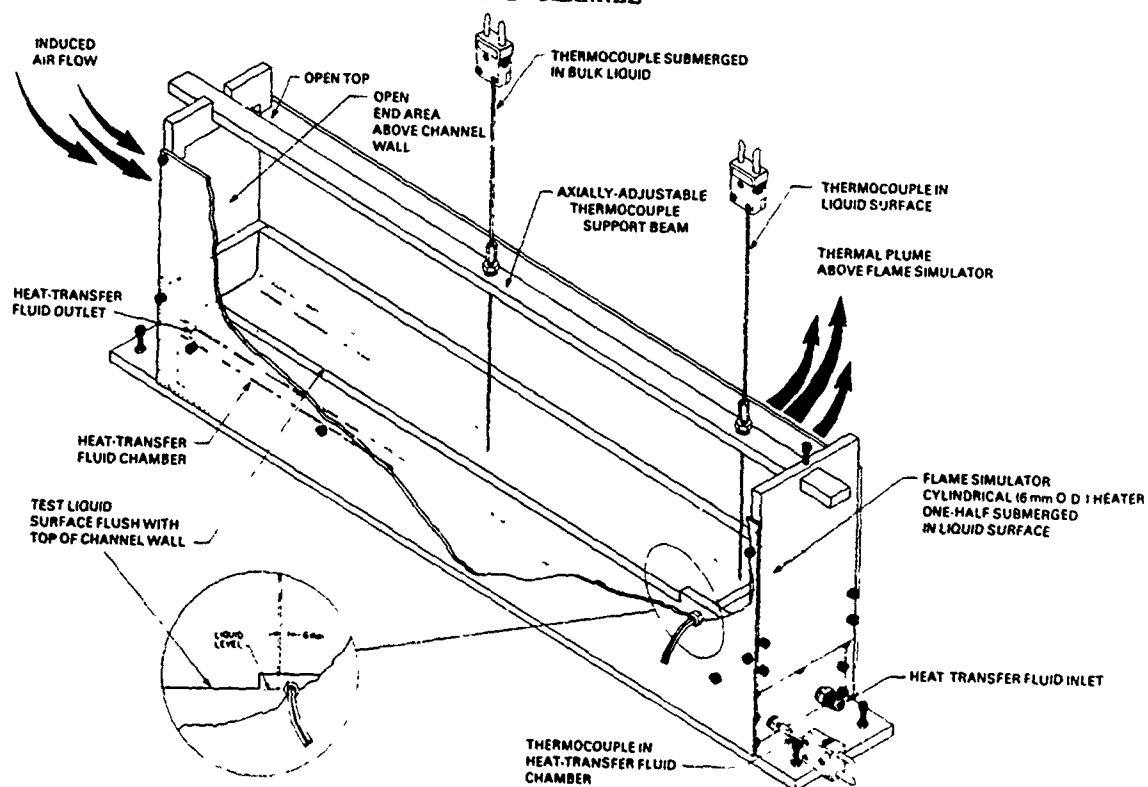


FIGURE 19. ANNOTATED ILLUSTRATION OF FLAME-PROPAGATION-SIMULATOR FUEL CHANNEL

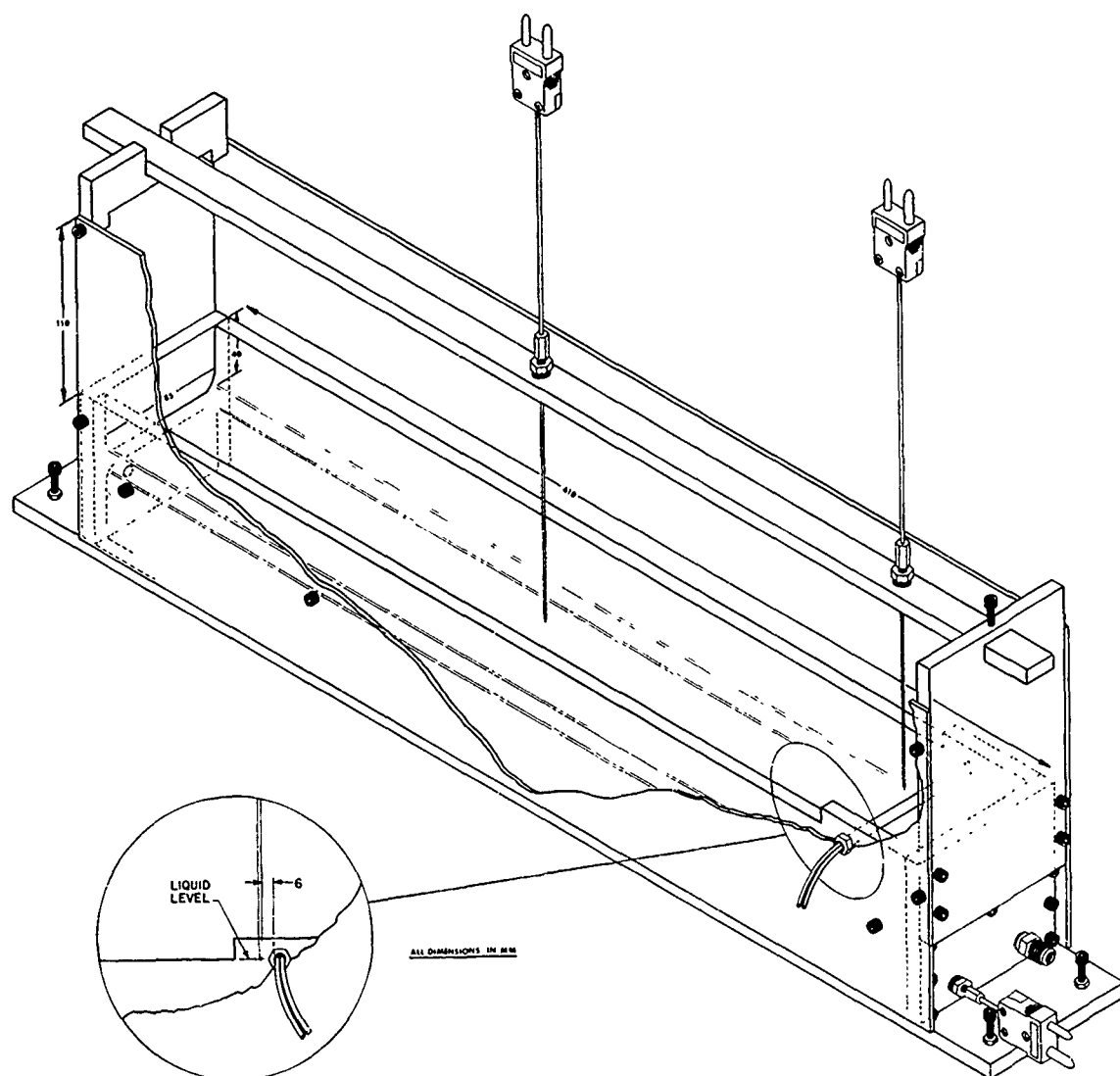


FIGURE 20. DIMENSIONAL DRAWING OF  
FLAME-PROPAGATION-SIMULATOR FUEL CHANNEL

flame simulator surface. Preliminary experiments indicated that the average surface heating rate does not change for thermocouple positions ranging from 3 mm to 25 mm distance from the flame simulator heater. The quasi-equili-

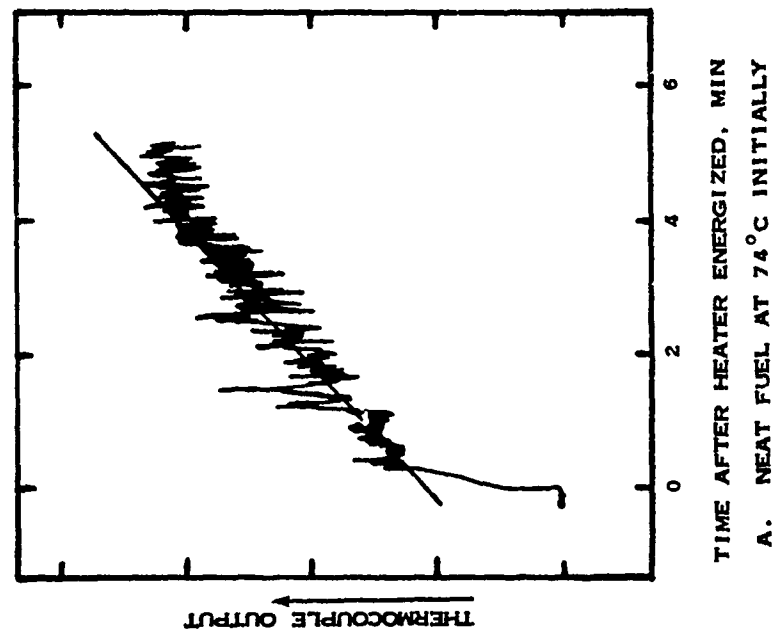
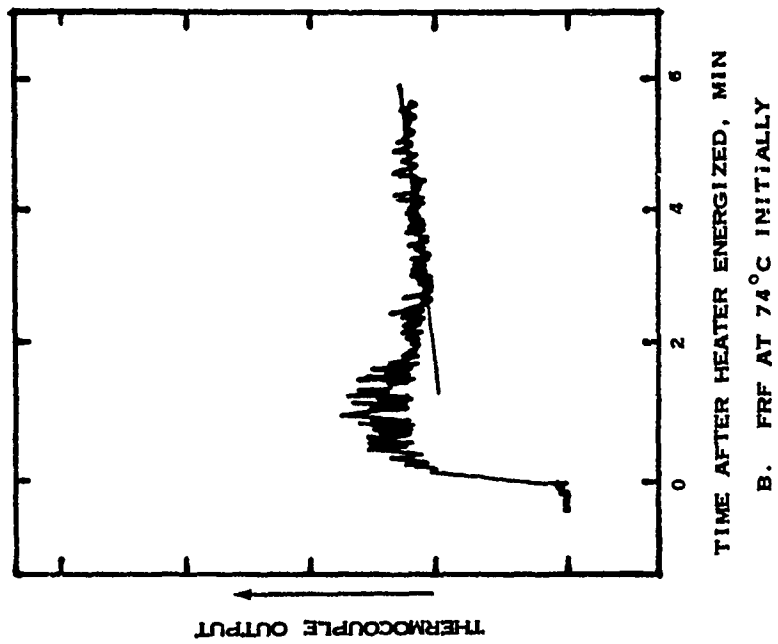


FIGURE 21. TYPICAL STRIP CHART RECORDER TRACES OF LIQUID SURFACE TEMPERATURE NEAR FLAME SIMULATOR IN FUEL CHANNEL

brium surface temperature is the steady-state average temperature indicated by the recorder trace after 5-10 minutes.

Experiments were conducted with FRF and neat base fuel at initial bulk liquid temperatures ranging from 0 to 74°C, and the data are summarized in Table 6.

The effects of initial bulk liquid temperature on liquid surface heating rates of neat fuel and FRF are shown in Figures 22 and 23. These effects are more pronounced with FRF than with neat fuel, and they indicate substantial influences of high viscosity at 0°C and significant evaporative cooling and/or surface-tension-gradient effects at bulk liquid temperatures above about 50°C.

In Figures 24 and 25 the steady-state liquid surface temperature is shown to increase with increasing initial bulk liquid temperature. The fact that the steady-state surface temperature of FRF is lower than that of neat base fuel when the initial bulk liquid temperature is greater than about 30°C provides strong evidence that surface evaporative cooling contributes to the horizontal flame propagation characteristics of FRF. The FRF surface temperature approaches a constant value of about 58°-66°C as the initial bulk liquid temperature is decreased and is higher than that of neat diesel fuel below about 15°C.

Figure 26 graphically portrays the direct influence of water content on the liquid surface heating rate of aqueous diesel fuel microemulsions/micellar solutions at 77°C. It is of particular interest that the apparent attenuation of the surface heating rate by increasing liquid water content between 0.5 and 10 vol% water parallels increasing water vapor pressure in a similar water composition range (Figure 10). Actually, this is not unexpected since the rate of evaporation from a liquid surface is proportional to the vapor pressure on the liquid side of the gaseous boundary layer.(7)

TABLE 6. FUEL CHANNEL TRANSIENT DATA

Fuel	Bulk Fuel (1)		Initial Vapor Pressure, atm(2)		Surface Heating Rate(3), °C/min	Quasi-Equilibrium Surface Condition (4)		
	Temperature, °C		Base Fuel	Water in FRF		Temp, °C	Vapor Pressure atm(2)	Excess Temp(5), °C
	Initial	Final						
DF-2*	74	79	0.04	---	6	107	0.07	28
0.5% H <sub>2</sub> O**	73	76	0.04	0.2	6	102	0.2	26
1.0% H <sub>2</sub> O**	74	78	0.04	0.2	5	101	0.2	23
5.0% H <sub>2</sub> O**	74	78	0.04	0.3	2	88	0.3	10
FRF*** <sup>2</sup>	74	77	0.04	0.3	0.6	83	0.5	6
H <sub>2</sub> O	73	74	--	--	-0.1	88	0.7	14
DF-2	70	73	0.04	---	6	103	0.06	30
DF-2	70	72	0.04	--	6	102	0.06	30
DF-2	69	72	0.04	---	6	103	0.06	31
DF-2	69	72	0.04	---	6	--	--	--
DF-2	--	70	0.04	---	6	104	0.06	34
DF-2	69	71	0.04	---	6	104	0.06	33
DF-2	69	71	0.04	---	6	--	--	--
FRF	69	72	0.04	0.2	0.8	84	0.5	12
FRF	71	72	0.04	0.2	0.7	83	0.5	11
FRF	--	70	0.04	0.2	0.7	81	0.4	11
DF-2	--	68	0.03	---	6	--	--	--
DF-2	62	63	0.03	---	6	86	0.05	23
DF-2	58	64	0.03	---	7	92	0.05	28
FRF	63	63	0.03	0.2	2	74	0.3	11
FRF	58	62	0.03	0.2	2	77	0.3	15
DF-2	45	48	0.02	--	7	83	0.05	35
DF-2	46	51	0.02	--	7	77	0.04	26
FRF	44	47	0.02	0.1	6	--	--	--
FRF	46	49	0.02	0.1	6	76	0.3	27
H <sub>2</sub> O	45	47	--	--	0.2	77	0.4	30
FRF	28	31	0.01	0.03	6	63	0.2	32
FRF	28	32	0.01	0.03	7	67	0.2	35
DF-2	18	24	(0.005)	--	7	65	0.2	41
FRF	18	24	(0.005)	(0.02)	6	67	0.2	43
DF-2	9	14	(0.003)	---	6	53	0.1	39
FRF	9	14	(0.003)	(0.01)	7	59	0.1	45
FRF	9	14	(0.003)	(0.01)	6	65	0.2	45
DF-2	0	8	(0.002)	---	6	47	0.1	39
DF-2	0	8	(0.002)	---	6	46	0.1	38
FRF	2	7	(0.002)	(0.01)	10	66	0.2	59
FRF	2	7	(0.002)	(0.01)	11	65	0.2	58

(1) Thermocouple immersed in center of channel.

(2) Correlated data of this project (data in parentheses are extrapolated).

(3) Maximum linear slope.

(4) Steady values 5-10 minutes after heater energized (185 watts).

(5) Surface temperature (6 mm from semi-submerged heater) minus bulk temperature, both 5 minutes after heater energized.

\*DF-2, Code 8821

\*\*Various water contents in 84/6 (v/v) base fuel/surfactant mixture.

\*\*\*FRF signifies 10 vol% water in 84/6 (v/v) base fuel/surfactant mixture.

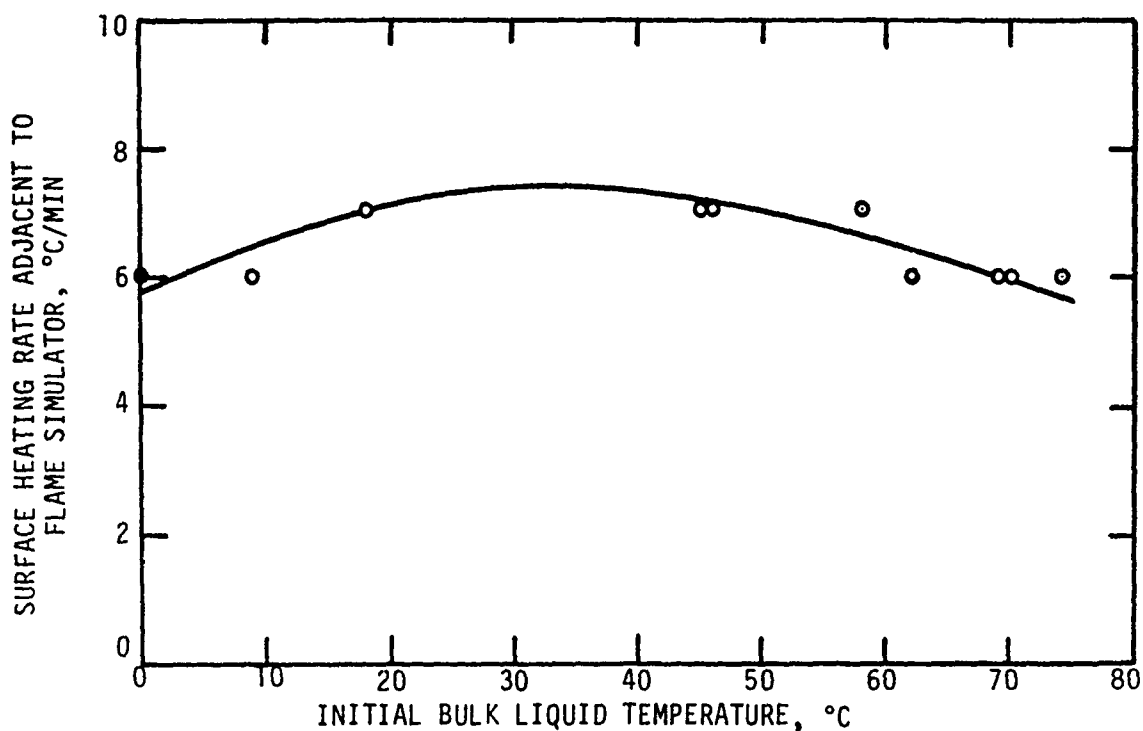


FIGURE 22. INFLUENCE OF NEAT DIESEL FUEL INITIAL TEMPERATURE ON SURFACE HEATING RATE ADJACENT TO FLAME SIMULATOR

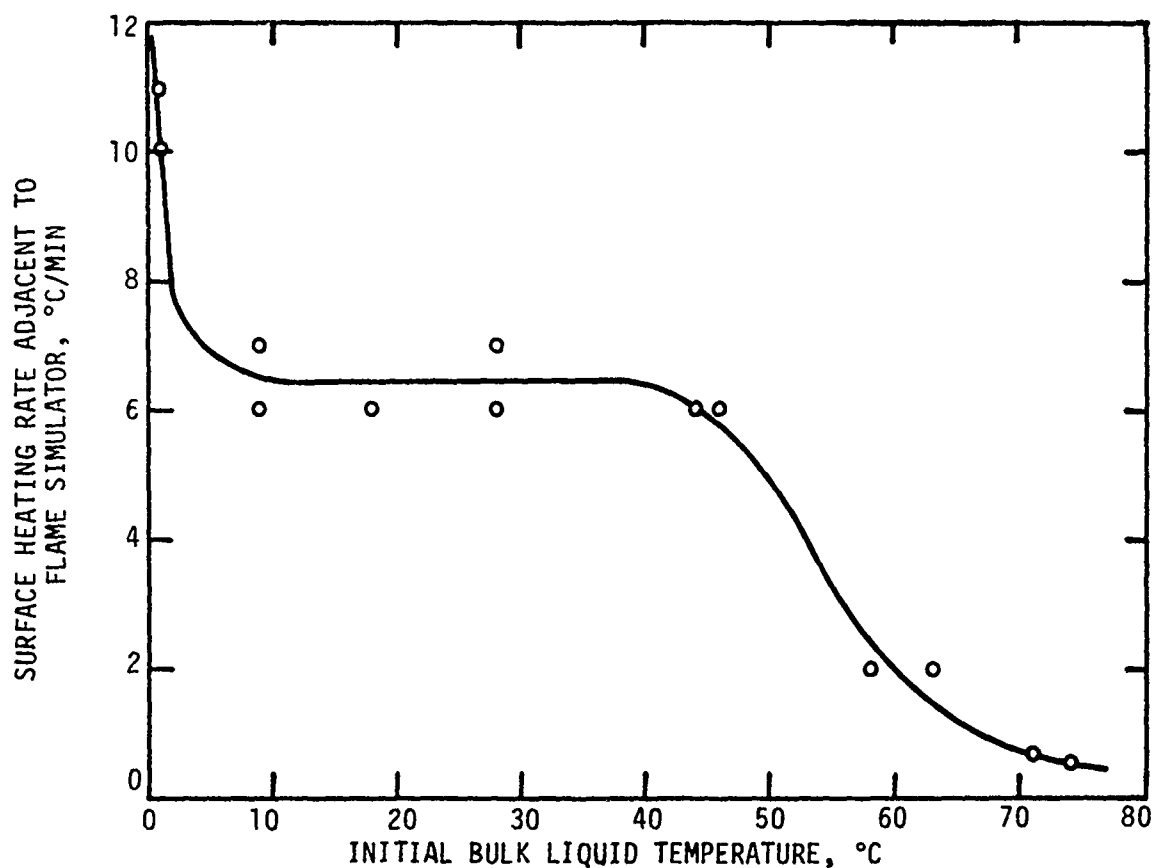


FIGURE 23. INFLUENCE OF FRF INITIAL TEMPERATURE ON SURFACE HEATING RATE ADJACENT TO FLAME SIMULATOR

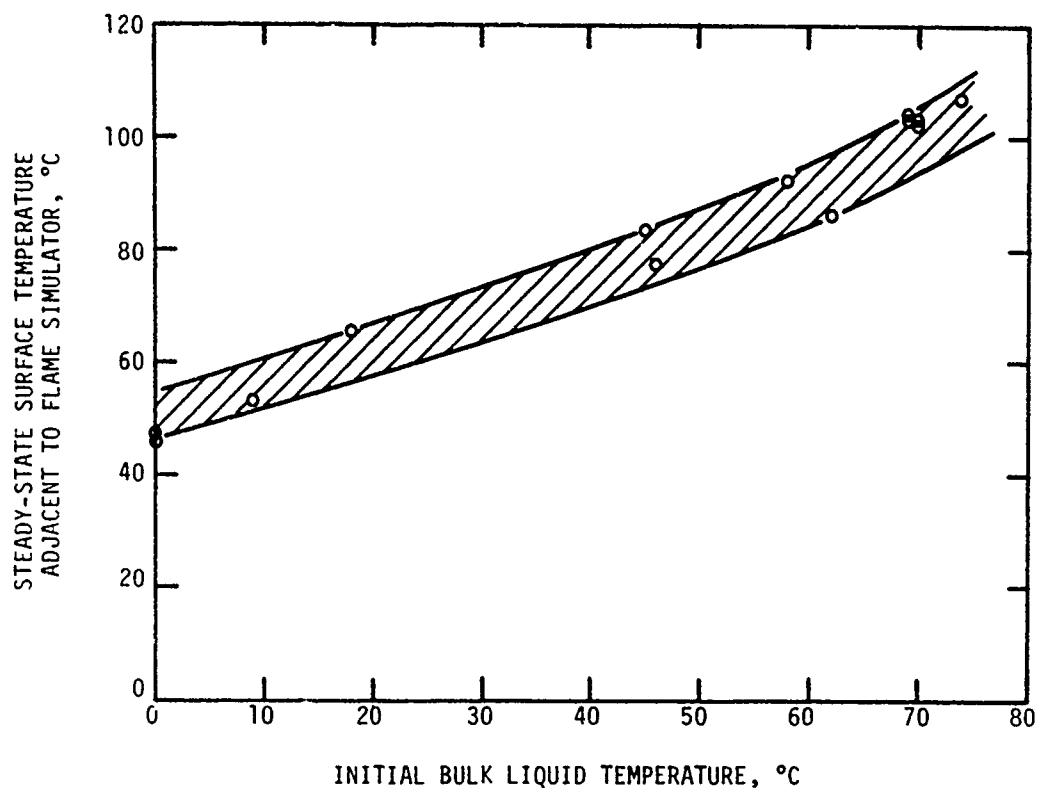


FIGURE 24. INFLUENCE OF NEAT FUEL INITIAL TEMPERATURE ON STEADY-STATE SURFACE TEMPERATURE ADJACENT TO FLAME SIMULATOR

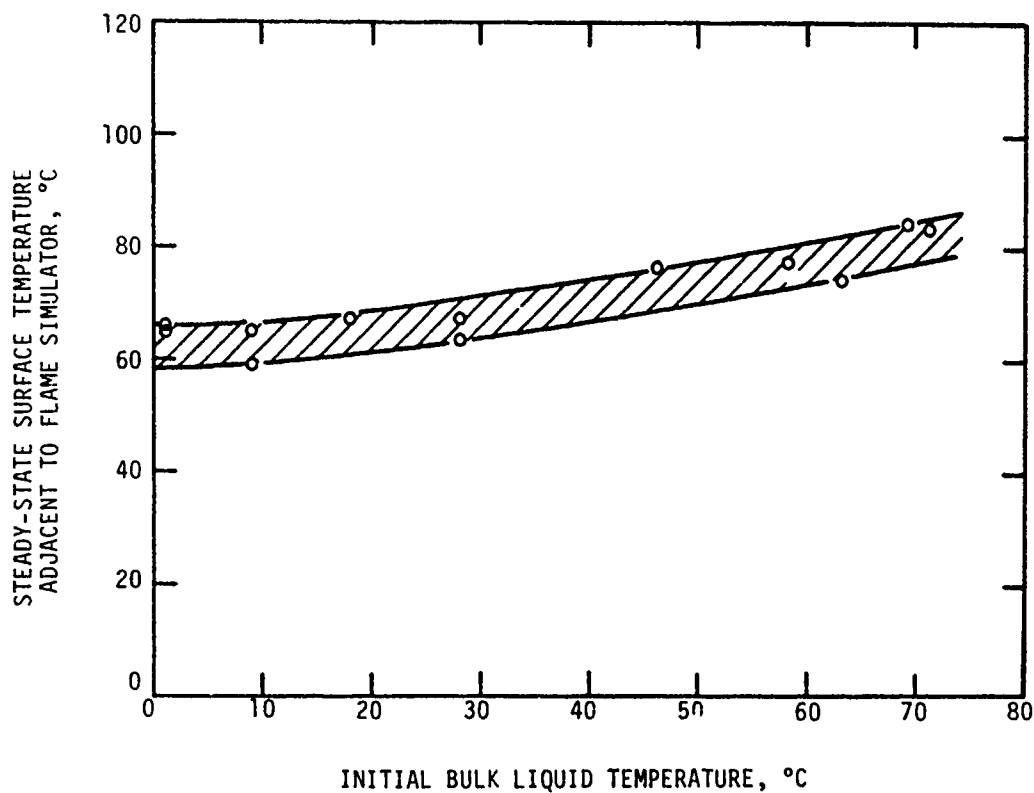


FIGURE 25. INFLUENCE OF FRF INITIAL TEMPERATURE ON STEADY-STATE SURFACE TEMPERATURE ADJACENT TO FLAME SIMULATOR

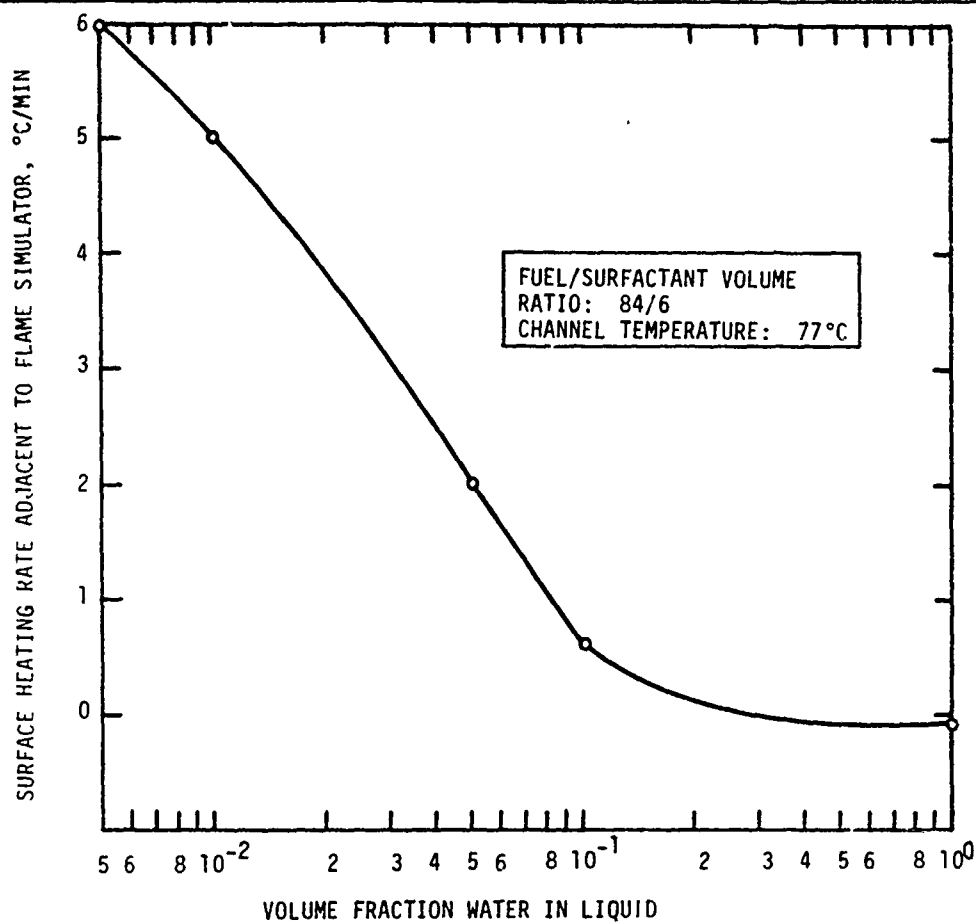


FIGURE 26. INFLUENCE OF INITIAL WATER CONTENT OF AQUEOUS DIESEL FUEL BLENDS ON SURFACE HEATING RATE ADJACENT TO FLAME SIMULATOR

## III. DISCUSSION

### A. Inter-relationships Among Observed Vapor Pressure, Flammability Limits, Flash Points, and Pool Flame Propagation

The correlated vapor pressure data of Figure 10 for 77°C are shown in Figure 27. As demonstrated by these data, the equilibrium water vapor partial pressure over FRF liquids containing varying amounts of water exhibits significant concentration dependence and is substantially less than the vapor pressure of pure water. The equilibrium water vapor pressure data for less than 1-2 vol% water in the liquid are linear in this semilog plot, and the data for more than 1-2 vol% water extrapolate linearly in this plot to the



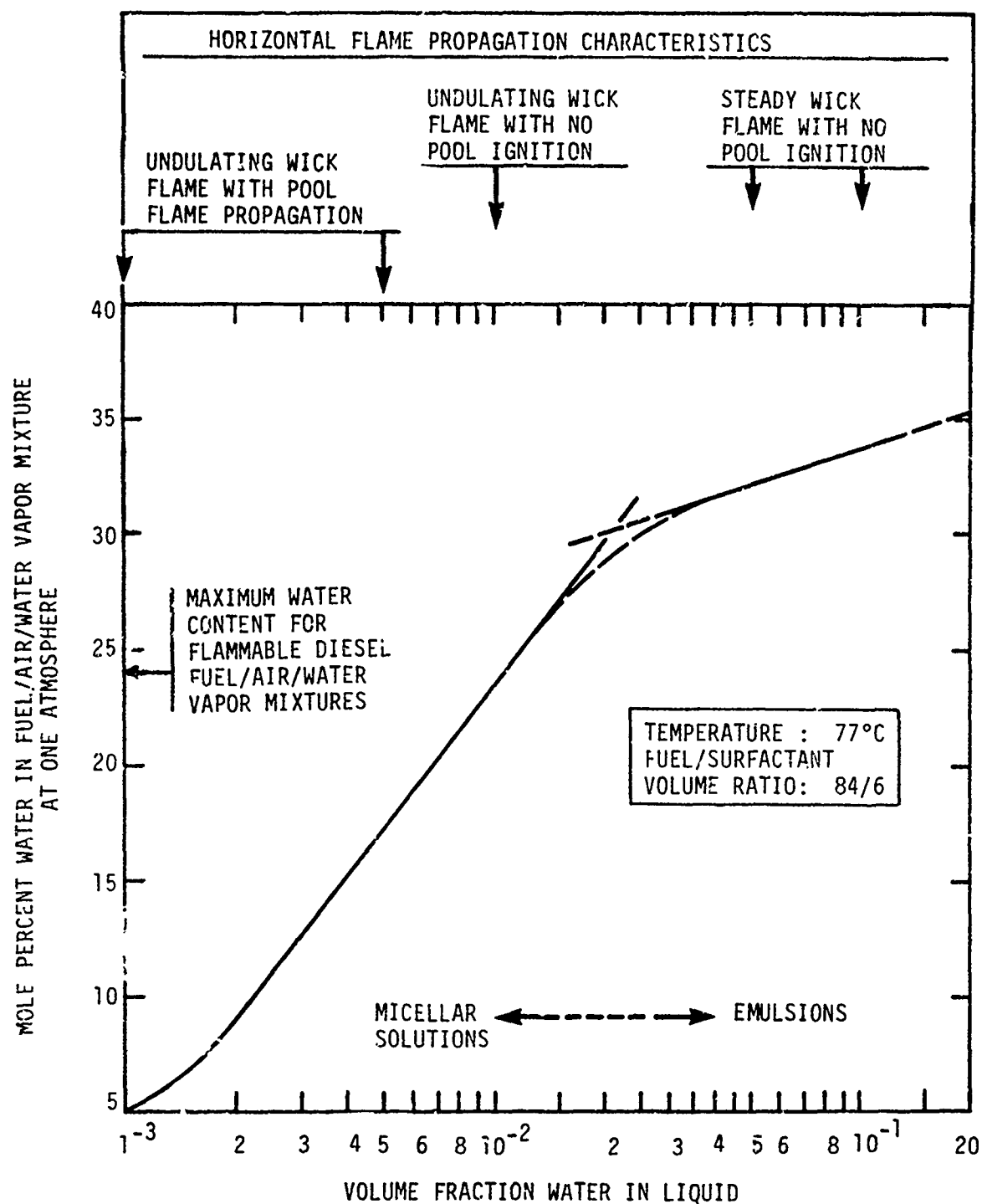


FIGURE 27. EQUILIBRIUM VAPOR COMPOSITION AND FLAMMABILITY PROPERTIES VERSUS FRF WATER CONTENT

value for 100 percent liquid water (100 percent not shown). The transitions in slope between these linear regions of the plots suggests a transition in the nature of the liquid phases. It should be noted that if these various blends behaved as true immiscible systems, the value for pure liquid water would have been observed in each case; hence, all of these liquids appear to behave as "nonideal solutions" rather than as immiscible systems.

These observed transitions in slopes between high water concentrations and low water concentrations are not in disagreement with published observations. It has been predicted theoretically (8) and observed experimentally (9,10) in isooctane/aerosol OT/water systems that when the volumetric ratio of surfactant to water is more than about 4, the systems behave as micellar solutions. In such solutions, the polar heads of the surfactant molecules are interlinked by hydrogen bonding, via bound water, forming "swollen" micelles.(9) With larger volumes of added water, a discrete water phase is present within each surfactant-surrounded droplet, and the systems behave as either microemulsions or macroemulsions, depending on the amount of water present and other system parameters\*. With FRF-type systems, the above-mentioned surfactant-water ratio of 4 lies within the slope transition region of Figure 27. Hence, this transition could correspond to a transition between microemulsions and micellar solutions.

The results of pool flame propagation experiments are also superposed in Figure 27. The peak flammability of 24 mole percent water vapor derived from the composite plot of Figure 8 is also shown in Figure 27 where it displays quantitative agreement with the indicated pool flame propagation results. FRF-type blends having equilibrium vapors containing less than 24

\*Microemulsions are kinetically or thermodynamically stable dispersions of surfactant-sheathed droplets. The droplet dimensions are in the same range as very large molecules and they experience Brownian motion.(9) Because of the small size of the droplets relative to the wave length of light, microemulsions range in appearance from transparent to translucent. Macroemulsions, on the other hand, are opaque suspensions of larger droplets which may experience sedimentation.(11) The properties of the droplet interfaces approach those of the droplet liquid rather than those of a surfactant sheath as in the case of microemulsions. Hence, the thermophysical properties of macroemulsions approach those of mixed immiscible phases.(4)

percent mole water exhibit pool flame propagation whereas those producing higher water-content vapors do not. In fact, the case where the liquid contains 1 vol% water (24 mole% water in the equilibrium vapor) displayed an undulated wick flame which was almost capable of departing from the wick, whereas the wick flame was steady for FRF-type blends containing 5 liquid vol% or more water.

Combining the correlations of Figures 8 and 14 yields the correlation shown in Figure 28. This derived flammability diagram correlates the liquid surface temperature of aqueous diesel fuel microemulsions with the measured vapor flammability characteristics. It represents an alternative flammabil-

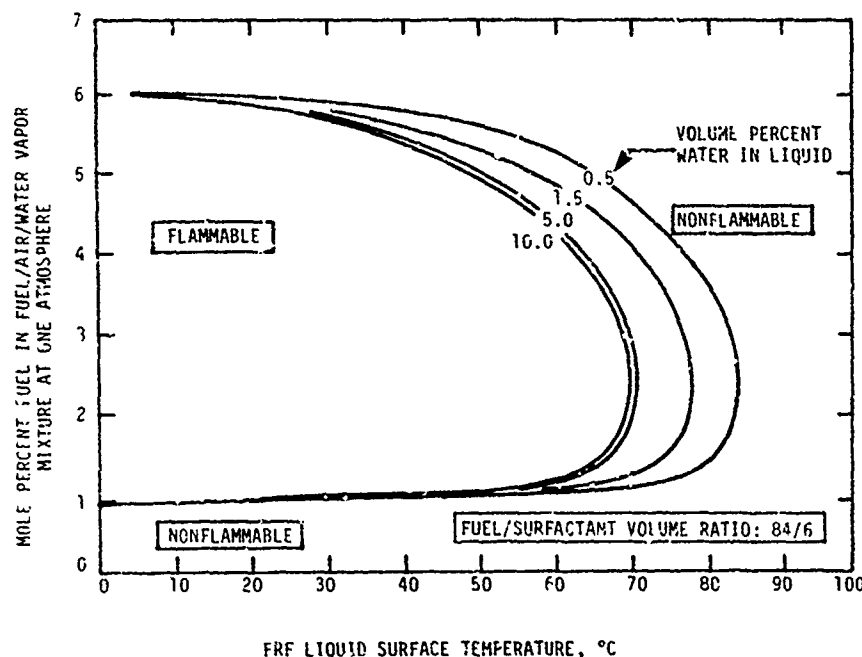


FIGURE 28. EQUILIBRIUM FLAMMABILITY DIAGRAM FOR FRF-TYPE FUEL-WATER BLENDS AT ONE ATMOSPHERE

ity diagram with which the absence of measurable FRF flash points above 70°C can be directly explained. Moreover, this correlation of liquid surface temperature with flammable vapor compositions, all well below 100°C, rules out the "phase rule" 100°C maximum surface temperature mechanism postulated in the literature.(4)

The data of Figure 28 indicate that FRF blends at temperatures less than about 70°C should not be self-extinguishing. However, results of the simulated pool flame experiments provide a satisfactory explanation of the FRF self-extinguishment which has been observed in AFLRL ballistic tests at temperatures down to about 20°C (ballistic tests were not conducted at lower temperatures). The leveling-out of surface temperatures at 58°-66°C with decreasing bulk liquid temperatures shown in Figure 25 indicates that the higher viscosities of FRF at lower temperatures\*, and/or other rheological effects, retard convective heat transfer in the liquid surface. Therefore, the temperature of the liquid surface near the flame simulator remains high enough to produce the water vapor blanket required for self-extinguishment.

#### B. Ability of FRF to Burn in Mist Form and On Wicks

The self-extinguishing character of aqueous diesel fuel microemulsions is exhibited only in the pool-burning mode where the fuel/air/water vapor mixture composition is determined by partial vaporization controlled by the volatility characteristics of the ingredients of the liquid fuel/water mixture. Self-extinguishment does not necessarily occur when the amount of air in the mixture can vary independently. For example, in the case of total vaporization of droplets of fuel/water mixture or total vaporization from a wick, flammable mixtures can result even when the fuel/air/water vapor mixture which would exist adjacent to the bulk liquid surface at the same temperature would be too rich in fuel vapor or water vapor to support combustion.

This phenomenon is best understood within the framework of a typical hydrocarbon flammability diagram such as that illustrated qualitatively in Figure 29. After a droplet is totally vaporized, or a fuel/water mixture is vaporized from a steady-state wick, the fuel/water ratio becomes fixed. As this

---

\*At temperatures from above 50°C to less than 20°C, the viscosity of FRF is normally about 50 percent greater than that of its base fuel. However, at 0°C, the FRF viscosity is more than twice that of its base fuel.

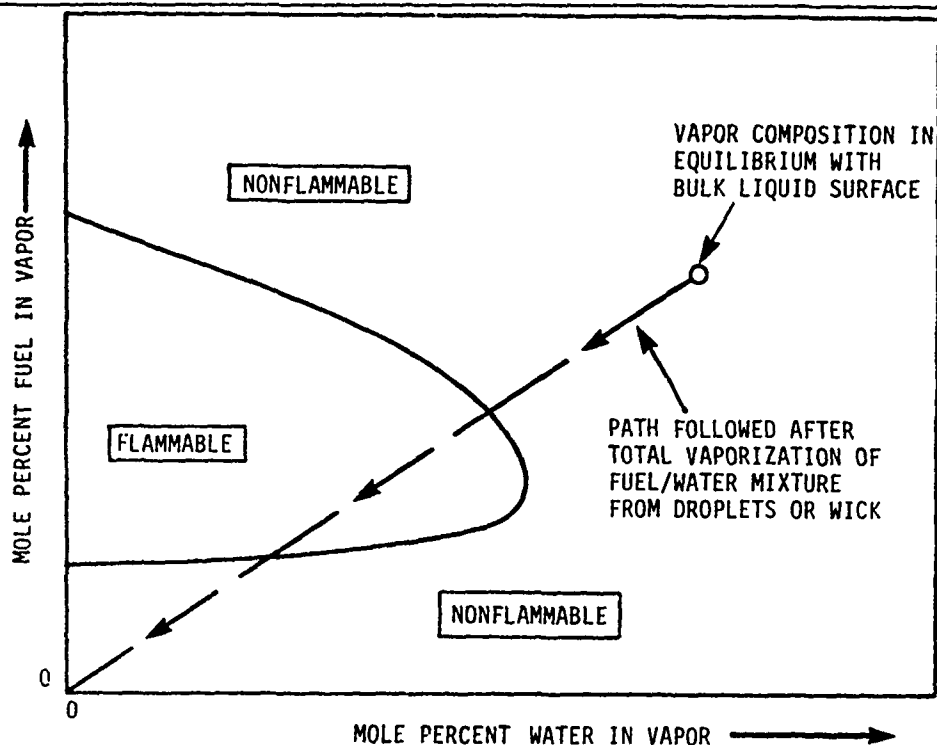


FIGURE 29. QUALITATIVE ILLUSTRATION OF TRANSITION  
FROM NONFLAMMABLE-TO-FLAMMABLE VAPORS  
AFTER TOTAL VAPORIZATION FROM A WICK OR OF MIST DROPLETS

vapor mixture is diluted with air, the water/fuel ratio does not change; therefore, its composition must follow a linear path which intersects the origin of the graph in Figure 29. A nonflammable vapor mixture thereby may become flammable upon mixing with air.<sup>(12)</sup> This behavior is consistent with the experimentally observed mist and wick flammability of FRF and with the external flashes observed when measuring the flash points of some FRF blends with high flash point base fuels ( $>70^{\circ}\text{C}$ ). The fact that FRF exhibits diminished mist flammability, relative to neat fuel, during ballistic and impact dispersion exposure modes may stem, at least in part, from such phenomena. Delays in ignition could result as the totally vaporized droplet mixes with air before its composition enters the flammable range.

#### IV. CONCLUSIONS

It has been established that the fire resistance exhibited by aqueous diesel

fuel microemulsions stems from the combination of mechanisms which are manifested as the nonflammable region of a water-vapor versus fuel-vapor composition diagram. The minimum pool surface temperature required for achieving such nonflammable vapor compositions has been established. It has been further established that the liquid surface in front of a flame attempting to propagate across a pool of FRF approaches this minimum temperature requirement regardless of the bulk liquid temperature (above 0°C). This minimum temperature could not have been predicted from basic principles because it was established by this study that the vapor pressure of FRF microemulsions is substantially less than it would be for classical immiscible water/fuel systems.

Equilibrium vapor pressure measurements indicate that FRF-type blends containing 6 vol% surfactant and between about 2 and 10 vol% water are microemulsions which exert equilibrium water partial pressures significantly less than that of pure water. When the water content is less than about 1 vol%, these systems appear to be micellar solutions with even lower equilibrium water partial pressures.

The experimentally-derived conclusions and the quantitative vapor pressure and vapor-phase flammability-limits data for water/diesel fuel microemulsions presented in this report represent substantial contributions to the literature in this area. The conclusions are summarized as follows.

#### Water Vapor Blanketing Is Shown to be the Predominant FRF Self-Extinguishment Mechanism

- Measurements of flammability limits of diesel fuel vapors in air diluted with various amounts of water vapor establish that such mixtures containing more than about 24 mole% water vapor cannot burn.
- Vapor pressure measurements confirm that FRF systems containing 10 vol% water are blanketed by equilibrium vapors containing at least 24 mole% water for liquid temperatures greater than about 70°C.
- The flash points of FRF blends containing 10 vol% water are about the same as those of the neat DF-2 fuel when the flash point is less than about 70°C. When the flash point of the base fuel exceeds 70°C, the

FRF does not exhibit a flash point. For these latter FRF blends, the partial vapor pressure of water is higher than the 24-mole-percent vapor phase composition limit for flammability.

#### Surface Thermophysical Effects Are Evident

- Evaporative cooling effects are significant, but they are not responsible for the self-extinguishing properties of FRF.
- Reduced convective heat transfer in the liquid surface results in preheating of the surface ahead of flame to 60°-70°C when bulk fuel temperature is as low as 0°C.

#### Pool Flame Propagation Results Indicate That as Low as 5 Vol % Water Content Can Prevent Sustained Ignition of FRF Liquid Surface, Depending Upon The Exposure

- Ballistic tests using 3.2-inch shaped charges showed FRF with 5 vol% water to be self-extinguishing.
- Ballistic tests using 20-mm HEIT rounds showed FRF with 5 vol% water to be non-self-extinguishing.

#### Specialized Experimental Equipment Developed for This Study Is Effective

- Vapor flammability apparatus
- Vapor pressure apparatus
- Surface thermophysical effects apparatus

### V. RECOMMENDATIONS

- The influence of FRF bulk fuel temperature on surface temperatures ahead of an actual flame should be studied.
- Exploiting the results of this investigation, a study should be conducted to examine the influence of alternate surfactant systems on the flammability mitigation characteristics of water-containing diesel fuel blends.

## VI. LIST OF REFERENCES

1. Weatherford, W.D., Jr., Fodor, G.E., Naegeli, D.W., Wright, B.R., Owens, E.C., and Schaekel, F.W., "Development of Army Fire-Resistant Diesel Fuel", prepared by Southwest Research Institute, U.S. Army Fuels and Lubricants Research Laboratory, under U.S. Army Contract Nos. DAAK70-78-C-0001 and DAAK70-80-C-0001, Interim Report AFLRL No. 111, December 1979 (DDC No. AD A083610); "Army Fire Resistant Diesel Fuel", presented at SAE Fuels and Lubricants Meeting, Houston TX, October 1979 (SAE Paper No. 790926).
2. Weatherford, W.D., Jr., Fodor, G.E., Kanakia, M.D., Naegeli, D.W., Wright, B.R., and Schaekel, F.W., "Research on Fire-Resistant Diesel Fuel", prepared by Southwest Research Institute, U.S. Army Fuels and Lubricants Research Laboratory, under U.S. Army Contract No. DAAK70-80-C-0001, Report AFLRL No. 145, December 1981 (DDC No. AD A117408).
3. Weatherford, W.D., Jr., discussion of "Halogenated Fire Extinguishants: Flame Suppression by a Physical Mechanism", by E.R. Larsen, ACS Symposium Series No. 16, "Halogenated Fire Suppressants", R.G. Gann, ed., 1975, pp 391-3.
4. Law, C.K., "Combustion Studies of Oil/Water Emulsions", prepared by Northwestern University, under U.S. Army Research Office Grant No. DAAG29-77-G-0188, Final Report, 30 September 1980; "On The Fire-Resistant Nature of Oil/Water Emulsions," Fuel, 60, 98-9 (1981).
5. Dryer, F.L., Glassman, I., Law, C.K., and McKay, R., personal communications, May 1980.
6. Zabetakis, M.G., "Flammability Characteristics of Combustible Gases and Vapors," USDoI, Bureau of Mines, Bulletin 627, 1965.
7. Spalding, D.B., "Some Fundamentals of Combustion," "Gas Turbine Series, Vol. 2," Butterworths Scientific Publications, London, 1955.
8. Ekwall, P., Mandell, L., and Kristen, F., "Some Observations on Binary and Ternary Aerosol OT Systems," J. Colloid Interface Sci., 33, 215 (1970).
9. Zulaf, M. and Eicke, H.F., "Inverted Micelles and Microemulsions in the Ternary System  $H_2O$ /Aerosol-OT/Isooctane as Studied by Photon Correlation Spectroscopy," J. Phys. Chem., 83, 480 (1979).



10. Mazer, N.A. et al., "Micellization, Solubilization, and Microemulsions," Vol. 1, K.L. Mittal, ed., Plenum Press, N.Y., 1977, p. 383.
11. Prince, L.M., "Microemulsions Theory and Practice," Academic Press, 1977, pp. 1, 2.
12. Gerstein, M. and Stine, W.B., "Anomalies in Flash Points of Liquid Mixtures," Ind. Eng. Chem., 12, 253-5 (1973).

## APPENDIX

### Fuel Properties

TABLE A-1. REFERENCE FUEL PROPERTIES

Property (Fuel Code)	(No. 7225)	(No. 8821) Fed. Spec.	(FRF of No. 8821)*	No. 9295)
Specification Type	MIL-F-46162A(MR)-II	VV-F-800b-DF-2	--	VV-F-800b-DF-A
Gravity, °API at 15.5°C	36.1	35.2	30.4	30.4
Density, g/mL at 15.5°C	0.844	0.848	0.874	0.795
Flash Point, °C(°F)	60(140)	72(161)	None	45(113)
Fire Point, °C(°F)	91(196)	84(183)	--	--
Cloud Point, °C(°F)	-21 (-6)	-1 (30)	--	-52 (126)
Pour Point, °C(°F)	-24 (-11)	-10 (14)	--	-56 (133)
Kinematic Viscosity, cSt at 40°C	2.2	3.2	5.3	1.2
Accelerated Stability				
(ASTM D 2274), mg/100 mL	0.6	2.7	--	--
Total Acid No., mg KOH/g	0.01	0.03	1.12	--
Steam Jet Gum, mg/100 mL	3.9	3.2	--	--
Sulfur, wt%	0.35	0.47	0.36	0.0
Nitrogen, wt%	--	--	-0.32	--
Copper Strip Corrosion				
(ASTM D 130)	1A	1A	--	1A
Carbon, wt%	86.8	86.7	75.06	--
Hydrogen, wt%	13.2	13.3	12.66	--
Heat of Combustion (Gross), J/kgx10 <sup>6</sup>	45.1	45.7	39.29	46.1
(Btu/lb)	(19,427)	(19,670)	(16,893)	(19,810)
Heat of Combustion (Net), J/kgx10 <sup>6</sup>	42.5	42.8	36.47	--
(Btu/lb)	(18,283)	(18,450)	(15,679)	--
Hydrocarbon Types, FIA, vol% saturates	--	69.1	--	87.3
aromatics	--	29.4	--	10.8
Hydrocarbon Types, HPLC, wt% saturates	72.5	74.1	--	--
aromatics	27.5	25.9	--	--
Aromatic Ring Carbon, UV, wt% mononuclear	7.1	7.5	--	5.5
dinuclear	11.5	6.5	--	2.4
trinuclear	0.3	0.4	--	0.0
total	18.9	14.4	--	7.9
Cetane No.	48	51	--	51
Distillation (ASTM D 86), °C(°F)				
Initial Boiling Point	166 (331)	183 (362)	--	164 (328)
10% Distilled	219 (426)	225 (437)	--	178 (353)
50% Distilled	244 (471)	282 (539)	--	191 (376)
90% Distilled	296 (565)	331 (628)	--	214 (418)
End Point	358 (676)	361 (682)	--	252 (485)

\*10 vol% water in 84/6 (v/v) base fuel/surfactant mixture.

TABLE A-2. PROPERTIES OF CITED FUELS

Property (Fuel Code)	(7931)	(7996)
Gravity, API° @ 15.5°C	33.8	35.3
Density, g/ml @ 15.5°C	0.856	0.848
Flash point, PMCC, °C(°F)	88(191)	68(155)
Distribution, ASTM D 86, °C(°F)		
IBP	223(433)	183(362)
5%	228(442)	209(408)
10%	233(452)	221(430)
15%	238(460)	230(446)
20%	243(470)	236(456)
30%	250(482)	246(474)
40%	252(486)	256(492)
50%	264(507)	263(506)
60%	273(523)	272(522)
70%	281(538)	282(540)
80%	290(554)	293(560)
90%	306(582)	310(590)
95%	318(604)	321(610)
EP	337(638)	333(632)

## LIST OF ABLREVIATIONS AND ACRONYMS

AFLRL: U.S. Army Fuels and Lubricants Research Laboratory  
ARO: U.S. Army Research Office  
ASTM: American Society for Testing and Materials  
DoD: Department of Defense  
FRF: Fire-resistant fuel  
HEIT: High explosive incendiary tracer round  
MERADCOM: Mobility Equipment Research and Development Command  
PCS: Photon correlation spectroscopy

# DISTRIBUTION LIST

## DEPARTMENT OF DEFENSE

DEFENSE DOCUMENTATION CTR 12  
CAMERON STATION  
ALEXANDRIA VA 22314

DEPT OF DEFENSE  
ATTN: DASA(MRA&L)-ES(MR DYKEMAN) 1  
WASHINGTON DC 20301

COMMANDER  
DEFENSE FUEL SUPPLY CTR  
ATTN: DFSC-T 1  
CAMERON STA  
ALEXANDRIA VA 22314

COMMANDER  
DEFENSE GENERAL SUPPLY CTR  
ATTN: DGSC-SSA 1  
RICHMOND VA 23297

## DEPARTMENT OF THE ARMY

HQ, DEPT OF ARMY  
ATTN: DALO-TSE 1  
DAMA-CSS-P (DR BRYANT) 1  
DAMA-ARZ (DR CHURCH) 1  
DAMA-SMZ 1  
WASHINGTON DC 20310

CDR  
U.S. ARMY MOBILITY EQUIPMENT  
R&D COMMAND  
Attn: DRDME-VF 10  
DRDME-WC 2  
FORT BELVOIR VA 22060

CDR  
U.S. ARMY MATERIAL DEVEL&READINESS  
COMMAND  
ATTN: DRCIDC (MR BENDER) 1  
5001 EISENHOWER AVE  
ALEXANDRIA VA 22333

CDR  
U.S. ARMY TANK-AUTOMOTIVE MATERIAL  
READINESS CMD  
ATTN: DRDTA-RG 1  
DRDTA-NS 1  
DRDTA-J 1  
WARREN MI 48090

CDR  
US ARMY TANK-AUTOMOTIVE MATERIAL  
READINESS CMD  
ATTN: DRSTA-G 1  
DRSTA-M 1  
DRSTA-GBP (MR MCCARTNEY) 1  
WARREN MI 48090

DIRECTOR  
US ARMY MATERIAL SYSTEMS  
ANALYSIS AGENCY  
ATTN: DRXSY-CM 1  
DRXSY-S 1  
DRXSY-L 1  
DRXSY-CR 1  
ABERDEEN PROVING GROUND MD 21005

CDR  
US ARMY APPLIED TECH LAB  
ATTN: DAVDL-ATL-ATP (MR MORROW) 1  
DAVDL-ATL 1  
FORT EUSTIS VA 23604

CDR  
US ARMY FORCES COMMAND  
ATTN: AFLG-RED (MR HAMMERSTROM) 1  
AFLG-POP (MR COOK) 1  
FORT MCPHERSON GA 30330

CDR  
US ARMY YUMA PROVING GROUND  
ATTN: STEYP-MT 1  
YUMA AR 85364

MICHIGAN ARMY MISSILE PLANT  
OFC OF PROJ MGR, XM-1 TANK SYS  
ATTN: DRCPM-GCM-S 1  
WARREN MI 48090

MICHIGAN ARMY MISSILE PLANT  
PROG MGR, FIGHTING VEHICLE SYS  
ATTN: DRCPM-FVS-SE 1  
WARREN MI 48090

PROJ MGR, M60 TANK DEVELOPMENT  
ATTN: DRCPM-M60-E 1  
WARREN MI 48090

PROG MGR, M113/M113A1 FAMILY  
OF VEHICLES  
ATTN: DRCPM-M113 1  
WARREN MI 48090

PROG MGR, MOBILE ELECTRIC POWER  
ATTN: DRCPM-MEP-TM 1  
7500 BACKLICK ROAD  
SPRINGFIELD VA 22150

CDK  
U.S. ARMY EUROPE & SEVENTH ARMY  
ATTN: AEAGC-FMD 1  
APO NY 09403

CDR  
THEATER ARMY MATERIAL MGMT  
CENTER (200TH)  
DIRECTORATE FOR PETROL MGMT  
ATTN: AEAG-MM-PT-Q (MR PINZOLA) 1  
ZWEIBEUCKEN  
APO NY 09052

CDR  
U.S. ARMY RESEARCH OFC  
ATTN: DRXRO-EG (DR SINGLETON) 1  
(DR. MANN) 1  
DRXRO-CB (DR. GHIRARDELLI) 1  
(DR. SQUIRE) 1  
P.O. BOX 12211  
RSCH TRIANGLE PARK NC 27709

DIR  
U.S. ARMY R&T LAB  
ADVANCED SYSTEMS RSCH OFC  
ATTN: MR. D. WILSTED 1  
AMES RSCH CTR  
MOFFITT FIELD CA 94035

CDR  
U.S. ARMY FOREIGN SCIENCE & TECH  
CENTER  
ATTN: DRXST-MT1 1  
FEDERAL BLDG  
CHARLOTTESVILLE VA 22901

CDR  
DARCOM MATERIAL READINESS  
SUPPORT ACTIVITY (MRSA)  
ATTN: DRXMD-MS 1  
LEXINGTON KY

HQ, US ARMY T&E COMMAND  
ATTN: DRSTE-10-0 1  
ABERDEEN PROVING GROUND, MD 21005

HQ, US ARMY TROOP SUPPORT &  
AVIATION MATERIAL READINESS  
COMMAND  
ATTN: DRSTS-MFG (2) 1  
DRCPO-PDE (LTC FOSTER) 1  
4300 GOODFELLOW BLVD  
ST LOUIS MO 63120

DEPARTMENT OF THE ARMY  
CONSTRUCTION ENG RSCH LAB  
ATTN: CERL-EM 1  
P.O. BOX 4005  
CHAMPAIGN IL 61820

HQ  
U.S. ARMY TRAINING & DOCTRINE CMD  
ATTN: ATCD-SL (MAJ HARVEY) 1  
FORT MONROE VA 23651

DIRECTOR  
U.S. ARMY RSCH & TECH LAB (AVADCOM)  
PROPULSION LABORATORY  
ATTN: DAVDL-PL-D (MR ACURIO) 1  
21000 BROOKPARK ROAD  
CLEVELAND OH 44135

CDR  
U.S. ARMY NATICK RES & DEV CMD  
ATTN: DRDNA-YEP (DR. KAPLAN) 1  
NATICK MA 01760

CDR  
U.S. ARMY TRANSPORTATION SCHOOL  
ATTN: ATSP-CD-MS 1  
FORT EUSTIS VA 23604

CDR  
U.S. ARMY QUARTERMASTER SCHOOL  
ATTN: ATSM-CD-M 1  
ATSM-CTD-MS 1  
ATSM-TNG-PT (COL VOLPE) 1  
FORT LEE VA 23801

HQ, U.S. ARMY ARMOR SCHOOL  
ATTN: ATSB-TD 1  
FORT KNOX KY 40121

CDR  
U.S. ARMY LOGISTICS CTR  
ATTN: ATCL-MS (MR. A. MARSHALL) 1  
FORT LEE VA 23801

CDR  
U.S. ARMY FIELD ARTILLERY SCHOOL  
ATTN: ATSF-CD 1  
FORT SILL OK 73503

CDR  
U.S. ARMY ORDNANCE CRT & SCHOOL  
ATTN: ATSL-CTD-MS 1  
ABERDEEN PROVING GROUND MD 21005

CDR  
U.S. ARMY ENGINEER SCHOOL  
ATTN: ATSE-CDM 1  
FORT BELVOIR VA 22960

CDR  
U.S. ARMY INFANTRY SCHOOL  
ATTN: ATSH-CD-MS-M 1  
FORT BENNING GA 31905

CDR  
U.S. ARMY AVIATION CTR & FT RUCKER  
ATTN: ATZQ-D 1  
FORT RUCKER AL 36362

DEPARTMENT OF THE NAVY

CDR  
NAVAL AIR PROPULSION CENTER  
ATTN: PE-71 (MR. MAGETTI) 1  
PE-72 (MR. D'ORAZIO) 1  
P.O. BOX 7176  
TRENTON NJ 06828

CDR  
NAVAL SHIP ENGINEERING CTR  
CODE 6101F (MR R. LAYNE) 1  
WASHINGTON DC 20362

CDR  
DAVID TAYLOR NAVAL SHIP R&D CTR  
CODE 2830 (MR. G. BOSMAJIAN) 1  
CODE 2831 1  
ANNAPOLIS MD 21402

DEPARTMENT OF THE NAVY  
HQ, U.S. MARINE CORPS  
ATTN: LPP (MAJ SANBERG) 1  
LMM (MAJ GRIGGS) 1  
WASHINGTON DC 20380

CDR  
NAVAL RESEARCH LABORATORY  
ATTN: CODE 6170 (MR. H. RAVNER) 1  
CODE 6180 (DR. CARHART) 1  
CODE 6110 (DR. HARVEY) 1  
WASHINGTON DC 20375

CHIEF OF NAVAL RESEARCH  
ATTN: CODE 473 (DR R. MILLER) 1  
ARLINGTON VA 22217

CDR  
NAVAL AIR ENGR CENTER  
ATTN: CODE 92727 1  
LAKEHURST NJ 08733

CDR,  
NAVAL MATERIAL COMMAND  
ATTN: MAT-C8T3 (DR. A. ROBERTS) 1  
CP6, RM 606  
WASHINGTON DC 20360

CDR  
U.S. AIR FORCE WRIGHT AERONAUTICAL  
LAB  
ATTN: /FWAL/POSF (MR. CHURCHILL) 1  
/FWAL/POSL (MR. JONES) 1  
AFWAL/POSH (MR. CLODFELTER) 1  
WRIGHT-PATTERSON AFB OH 45433

CDR  
AIR FORCE OFFICE OF SCIENTIFIC  
RESEARCH  
ATTN: (DR. JULLIAN) 1  
BOLLING AFB  
WASHINGTON DC 20332

CDR  
USAF SAN ANTONIO AIR LOGISTICS  
CTR  
ATTN: SAALC/SFQ (MR MAKRIS) 1  
SAALC/MMPRR (MR ELLIOT) 1  
KELLEY AIR FORCE BASE, TX 78241

CDR  
U.S. AIR FORCE WRIGHT AERONAUTICAL  
LAB  
ATTN: AFWAL/MLSE (MR MORRIS) 1  
AFWAL/MLBT 1  
WRIGHT-PATTERSON AFB OH 45433



CDR  
USAF WARNER ROBINS AIR LOGISTIC  
CTR  
ATTN: WR-ALC/MMIRAB-1 (MR GRAHAM) 1  
ROBINS AFB GA 31098

OTHER GOVERNMENT AGENCIES

U.S. DEPARTMENT OF TRANSPORTATION  
ATTN: AIRCRAFT DESIGN CRITERIA  
BRANCH 1  
FEDERAL AVIATION ADMIN  
2100 2ND ST SW  
WASHINGTON DC 20590

U.S. DEPARTMENT OF TRANSPORTATION  
FEDERAL AVIATION ADMINISTRATION  
ATTN: T.G. HOREFF, AWS-120 2  
800 INDEPENDENCE AVE  
WASHINGTON DC 20591

U.S. DEPT OF TRANSPORTATION  
NATIONAL AVIATION FACILITIES  
EXPERIMENTAL CENTER  
ATTN: W. WESTFIELD 1  
ATLANTIC CITY NJ 08405

U.S. ARMY BALLISTICS RESEARCH LAB  
DXDAR-BLT-T (MR. COPELAND)  
ABERDEEN PROVING GROUND, MD 21005 1

U.S. DEPARTMENT OF COMMERCE  
NATIONAL BUREAU OF STANDARDS  
ATTN: (DR. SNELL) 2  
WASHINGTON DC 20234

U.S. DEPARTMENT OF ENERGY  
DIV OF TRANS ENERGY CONSERV 2  
ALTERNATIVE FUELS UTILIZATION  
BRANCH  
20 MASSACHUSETTS AVENUE  
WASHINGTON DC 20545

SCI & TECH INFO FACILITY  
ATTN: NASA REP (SAK/DL) 1  
P.O. BOX 8757  
BALTIMORE/WASH INT AIRPORT MD 21240

PROF. C.K. LAW  
NORTHWESTERN UNIVERSITY 1  
DEPT. OF MECH. ENGR.  
EVANSTON IL 60201

PROF RAYMOND MACKAY  
DREXEL UNIVERSITY  
DISGUE HALL, ROOM 224 1  
32ND ST. AT CHESTNUT AND MARKET  
PHILADELPHIA PA 19104

PROF. I. GLASSMAN  
PRINCETON UNIVERSITY 1  
DEPT. OF MECH & AEROSPACE ENGR.  
ENGINEERING QUADRANGLE  
PRINCETON NJ 08544

PROF. F.L. DRYER  
PRINCETON UNIVERSITY 1  
DEPT. OF MECH. AND AEROSPACE ENGR.  
ENGINEERING QUADRANGLE, D-329a  
PRINCETON NJ 08544